

Accepted Manuscript

Cockade breccia: Product of mineralisation along dilational faults

Max Frenzel, Nigel H. Woodcock

PII: S0191-8141(14)00198-9

DOI: [10.1016/j.jsg.2014.09.001](https://doi.org/10.1016/j.jsg.2014.09.001)

Reference: SG 3117

To appear in: *Journal of Structural Geology*

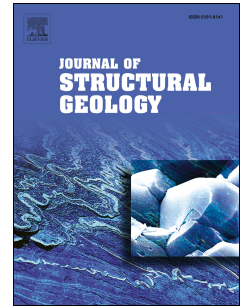
Received Date: 6 June 2014

Revised Date: 29 August 2014

Accepted Date: 2 September 2014

Please cite this article as: Frenzel, M., Woodcock, N.H., Cockade breccia: Product of mineralisation along dilational faults, *Journal of Structural Geology* (2014), doi: 10.1016/j.jsg.2014.09.001.

This is a PDF file of an unedited manuscript that has been accepted for publication. As a service to our customers we are providing this early version of the manuscript. The manuscript will undergo copyediting, typesetting, and review of the resulting proof before it is published in its final form. Please note that during the production process errors may be discovered which could affect the content, and all legal disclaimers that apply to the journal pertain.



1
2
3
4
5
6
7
8
9
10
11
12
13
14
15

16 **Cockade breccia: product of** 17 **mineralisation along dilational faults**

18
19
20
21
22
23 by Max Frenzel^{a,*} and Nigel H. Woodcock^b

24
25
26
27 ^a Helmholtz-Institute Freiberg for Resource Technology, Halsbrücker Str. 34, 09599
28 Freiberg, Germany; E-mail: m.frenzel@hzdr.de; Tel.: +49 (0) 351 2604407

29
30 ^b Department of Earth Sciences, University of Cambridge, Downing Street, Cambridge,
31 CB2 3EQ, United Kingdom; E-mail: nhw1@cam.ac.uk; Tel.: +44 (0) 1223 333430

32
33 * Corresponding author

34
35
36 Keywords: cockade ore; ring ore; syntectonic mineralisation; dilational faulting; epithermal
37 veins

38 **Abstract**

39

40 Cockade breccias are a type of fault fills in which individual clasts are completely surrounded by
41 concentric layers of cement. They occur particularly in low-temperature near-surface hydrothermal
42 veins. At least six mechanisms have been proposed for the formation of cockade breccia-like
43 textures, but only two – repeated rotation-accretion, and partial metasomatic replacement of clast
44 minerals – have been supported by detailed evidence. A typical example of cockade breccia from
45 the Gower Peninsula (South Wales) shows clear evidence for the rotation-accretion mechanism: in
46 particular, overgrown breakage points in cement layers – where cockades were previously touching
47 each other – and rotated geopetal infills of haematitic sediment. Based on the available evidence, it
48 is proposed that cockade textures result from low rates of cement growth compared to high rates of
49 dilational fault slip. Seven criteria are given for the correct identification of cockade breccias.

50 1. Introduction

51

52 Fault zones are important in controlling fluid flow in the upper crust. Depending on the
53 permeability of the fault core and surrounding damage zone, an individual fault zone can act either
54 as a barrier or a conduit for fluids (Caine et al., 1996; Faulkner et al., 2010). Most fluids alter the
55 permeability of fault zones over time by deposition of mineral cements and reaction with the
56 wallrocks (e.g. Woodcock et al., 2007). Critical to understanding fault zones is the identification and
57 interpretation of fault rocks, particularly fault breccias: coarse fault rocks with potentially high
58 permeability.

59 Recent classification schemes for fault breccias (Mort and Woodcock, 2008; Woodcock and
60 Mort, 2008) are non-genetic and easily applicable in the field. However, they do not deal
61 satisfactorily with fault rocks dominated by crystalline cement. Rocks with less than 30% large (>
62 2mm) clasts and less than 30% fine matrix are classified as ‘fault veins’ (Woodcock and Mort,
63 2008, Fig. 5b). However, these cement-rich fault rocks include a puzzling type of ‘breccia’ in which
64 clasts appear to be completely surrounded by cement: a geometry which has no simple genetic
65 explanation. These cement-supported breccias are commonly termed ‘cockade breccias’.

66 The term cockade breccia (also: cockade ore, cockade texture) refers specifically to
67 hydrothermal fault fills in which centimetre- to decimetre-sized clasts appear to be completely
68 enclosed by concentric bands of cement (Bastin, 1950; Kutina and Sedlackova, 1961; Genna et al.,
69 1996; Leroy et al., 2000). Cockade breccias are of considerable interest in the study of vein-type
70 mineral deposits because they may record much of a vein’s mineralisation sequence (Leroy et al.,
71 2000) and provide evidence for syntectonic mineralisation (Van Alstine, 1944; Genna et al., 1996),
72 allowing correlation of mineralisation with deformation. Yet, there is no consensus on the exact
73 origin of cockade breccias, and some confusion exists in the literature about nomenclature and
74 identification. This paper therefore aims a) to summarise research on the formation of cockade
75 breccias, b) to present new evidence for the syntectonic formation of cockade textures in carbonate
76 vein fills on the Gower Peninsula, Wales, and c) to review nomenclature and classification of
77 cockade breccias, particularly to help their correct identification in the field and the laboratory.

78

79 2. History and usage of the term *cockade*

80

81 Cockade breccias were first described from Pb-Zn-Ag veins in the German part of the Erzgebirge
82 Mountains as *Sphärengestein* (German *sphere rock*; Weissenbach, 1836), although this term
83 apparently included varieties with only one generation of columnar cement. The terms *Kokardenerz*
84 (*cockade ore*) and *Ringelerz* (*ring ore*) used by Cotta (1859) and other authors (Pošepný, 1895;

85 Beck, 1903) to describe similar ore-bearing fissure fills refer to the concentric banding around
86 individual clasts seen in sections.¹ It is from the translation of Cotta's work on ore deposits that this
87 terminology seems to have entered English geological nomenclature (Cotta, 1870). Variants such as
88 *cocarde ore* also appear (Pošepný, 1895) but have not stood the test of time. Sperling (1973) gives
89 separate but overlapping definitions of the terms ring ore and cockade ore. He defines ring ore as an
90 end member of the transition from banded veins with straight bands to those with wavy, and finally
91 concentric bands, when overgrowing single wall rock fragments (calcite, sphalerite, galena).
92 Cockade ore, on the other hand, is defined by fine-grained, layered intergrowths of galena and
93 quartz overgrowing host-rock fragments. This distinction seems superficial since the resulting
94 textures are symmetrically and genetically equivalent. Cockade ores have also been called *orbicular*
95 or *nodular* ores by some authors (Spurr, 1926; Van Alstine, 1944; Penczak and Mason, 1997).

96 In a number of publications, mis-applications of the terms cockade breccia or cockade texture
97 deviating significantly from the original definition were encountered. For instance, breccias where
98 only a single generation of cement surrounds individual fragments are sometimes called cockade
99 breccias (Feitzinger and Paar, 1991; Hagemann et al., 1992; Feitzinger et al. 1995; Kontak et al.,
100 1999; Yilmaz et al., 2010), probably due to confusion with the earlier term *Sphärengestein*. Because
101 of their superficially similar appearance in section, colloform cavity fills have also occasionally
102 been called cockade breccias, particularly with reference to Mississippi-Valley-Type mineral
103 deposits (Clar, 1929; Jicha, 1951; Kalliokoski, 1965; Schneider et al., 2002; Okrusch et al., 2007;
104 Patrier et al., 2013). Other non-canonical applications include the use for oolites (Ilavsky et al.,
105 1991), peloids (Kucha et al., 1990), microscopic overgrowths of one mineral on another (Genkin et
106 al., 1998), tourmaline sprays in aplite dikes (Boriani et al., 1988), vugs (Suh and Dada, 1997;
107 Vishiti et al., 2013), and normal columnar or laminar cements growing on vein walls (Hodgson,
108 1989; Byrne and Harris, 1993; Fusswinkel et al., 2013, 2014).

109 Historically, the term cockade breccia or cockade texture was intended exclusively for
110 hydrothermal breccias in which individual clasts are surrounded by several generations of cement
111 and, to avoid confusion, its meaning should be restricted accordingly. A set of textural criteria which
112 should be met by any true cockade breccia is presented below.

113

114 **3. Mode of occurrence**

115

116 A summary of 106 reported occurrences of cockade breccias in different types of deposits (Table

¹ A cockade (French *cocarde*) is a symbol consisting of differently coloured concentric rings, used for recognition by many, particularly military, organisations around the world. In the past, they were also used to show the allegiance of the wearer to a political faction, most prominently during the French Revolution with the creation of the *cocarde tricolor*, now a popular symbol of France and the basis for the current French national flag.

117 1) shows that they are most often reported from low- to mid-temperature (typical formation
118 temperatures between 50 – 350°C), vein-style mineralisation thought to have formed in near-surface
119 environments. However, the clear prevalence of reports from ore-bearing veins is probably due to a
120 significant sampling bias towards the well-exposed occurrences encountered in mines. Sampling
121 bias might also be responsible for the apparent relative abundance in different types of mineral
122 deposits.

123 The presence of cockade breccias is often used to indicate space-filling processes – rather than
124 replacement – during mineralisation (e.g. Perelló, 1994; Liu et al., 2011). However, this
125 interpretation has been challenged in some cases where ore minerals replaced specific cement
126 generations or formed along the contacts between cement and clasts (Kutina and Sedlackova, 1961;
127 Rieder, 1969), leading to an appearance similar to that of cockades *sensu stricto*.

128

129 **4. Proposed formation mechanisms**

130

131 *4.1. Six possible mechanisms*

132 Successive deposition of several cement generations is required for the formation of cockade
133 breccias. The resultant volume of cement means that clasts seem not to touch each other and appear
134 to be suspended within the cement. This was already noted by Weissenbach (1836), and a number of
135 explanations have been put forward for this phenomenon since his first description:

136

137 1) *The cut effect* (Fig. 1a). Pošepný (1895) noted as early as 1895 that a lack of contact points
138 between clasts in any 2D section does not preclude contacts in 3D. Pošepný showed this for
139 a few specific cases by preparing serial sections of specimens showing no contact points at
140 their surface. Later experiments by Talmage (1929) also showed that there is a high
141 probability for sections through random, self-supporting structures to contain abundant
142 seemingly unsupported fragments.

143

144 2) *Crystallisation pressure* (Fig. 1b). The earliest explanation for a true suspension of clasts
145 within the cement was put forward by Weissenbach (1836) himself. He proposed that
146 fragments were pushed apart by the crystallisation pressure exerted on the clasts by minerals
147 precipitating between them. Many authors have repeated this hypothesis (Cotta, 1859; Beck,
148 1903; Taber, 1918; Lindgren, 1919; Bastin, 1950).

149

150 3) *Suspension in fluid* (Fig. 1c). Another early hypothesis was that clasts were suspended in a
151 fluid during the growth of the cements, either because of the high viscosity or density of that

fluid (Spurr, 1926), or due to its fast speed of ascent (Farmin, 1938). Recently, the hypothesis of highly viscous and dense mineralising fluids was re-invoked by Dill and Weber (2010), while Jobson et al. (1994) re-introduced the hypothesis of a violently ascending fluid to explain the occurrence of cockade breccias.

- 4) *Partial metasomatic replacement of clast minerals* (Fig. 1d). Partial inward replacement/alteration of clasts might result in a lack of contact points between the residual cores of the clasts (e.g. Bateman, 1924; Bastin, 1925). Later deposition of another mineral around the clasts might give the (superficial) appearance of concentric layers of cement. Kutina and Sedlackova (1961) as well as Rieder (1969) present evidence for such processes contributing to the formation of some cockade breccia-like textures.
- 5) *Infall of clasts during cementation* (Fig. 1e). Kutina and Sedlackova (1961) pointed out that an apparent suspension of clasts within the cement might also be achieved by the gradual accumulation of rock fragments in a fissure simultaneous with mineral deposition.
- 6) *Repeated rotation and accretion* (Fig. 1f). Van Alstine (1944) proposed that cockades form by repeated fracturing of a partially cemented breccia, mostly along the boundaries between individual clasts, in an extending fissure followed by growth of a partial layer of new cement. Although individual layers never completely enclose the clasts, the low spatial density of contact points leads to the appearance of complete concentric layers of cement, and to the suspension of clasts within the cement. Genna et al. (1996) recently presented evidence for the same mechanism, but without citing Van Alstine (1944). Van Alstine's contribution was also omitted by Kutina and Sedlackova (1961) in the most comprehensive review of cockade formation to date.

While the cut effect (1) clearly explains some cockade-like textures, there are many breccias where clasts are demonstrably *not* in contact with each other. In such cases, detailed evidence has only been presented for the partial metasomatic replacement mechanism (4) (Kutina and Sedlackova 1961) and the rotation-accretion mechanism (6) (Van Alstine, 1944; Genna et al., 1996). However, a detailed discussion of the textural implications of all of the above possibilities is usually lacking. Therefore, such a discussion follows in the subsequent paragraphs.

4.2. Crystallisation pressure hypothesis

If cockade breccias were formed by the action of crystallisation pressure on loose granular

187 aggregates (2), the resulting textures would depend on the surface energies of the minerals involved.
188 If the cockades and cement are composed of minerals with very similar surface energy and surface
189 energy anisotropy, faces on individual crystallites would not develop, except in the first generation
190 of cement that grew into open spaces. Successive cement generations would be expected to show
191 only anhedral textures, similar to those developed in crack-seal veins. By contrast, cements
192 containing minerals with significantly higher surface energy and surface energy anisotropy (e.g.
193 pyrite in quartz; cf. Spry 1969), should develop crystal faces projecting into *all* directions, except
194 where grains of the same mineral impinge on one another. The minerals with the lower surface
195 energy should again not show developed crystal faces (Spry, 1969). Although veins have been
196 described in which such textures are observed, and which might therefore have formed through the
197 action of crystallisation pressure (Wiltschko and Morse, 2001; Hilgers and Urai, 2005; Philipp,
198 2008; Noriel et al., 2010), cockades generally lack such textures. They instead show rims of crystals
199 with well-developed growth faces projecting outward from the central clasts (e.g. Spurr, 1926;
200 Leroy et al., 2000). This indicates formation by growth into open spaces. The crystallisation
201 pressure hypothesis can therefore be dismissed on textural grounds.

202

203 4.3. *Fluid suspension hypothesis*

204 Two distinct cases require separate consideration: a) involvement of a highly viscous and dense
205 (drilling fluid-like) fluid agitated by fault movement (shear fluidisation) and b) involvement of a
206 low viscosity fluid at high flow speeds.

207 If indeed highly viscous drilling-fluid like suspensions were involved in the formation of
208 cockade breccias (as proposed by Dill and Weber, 2010), large amounts of fine-grained sediment
209 should be associated with the cockades – at least 20 vol.%. Although Dill and Weber (2010) do
210 report the occurrence of argillaceous material in normal breccia units, they fail to show its
211 association with the cockade material. Virtually all other occurrences of cockade breccias reported
212 in the literature show no association to fine-grained material, and the spaces between clasts are
213 usually filled by cement (e.g. Spurr, 1926; Buerger and Maury, 1927). Another reason to reject this
214 model is based on its implication that clasts remain suspended in the fluid for the entire duration of
215 cement growth. This is an unrealistic scenario, since the seismic agitation required to sustain the
216 drilling-fluid like suspension is intermittent and clasts should settle during interseismic periods.
217 Compaction and cementation would likely follow and result in a material difficult or impossible to
218 resuspend. Therefore, the drilling-fluid model is neither strongly supported by field evidence, nor
219 by general considerations of fault dynamics.

220 To evaluate rapidly ascending, low-viscosity aqueous fluids, analysis is needed of the
221 hydrodynamic conditions required to suspend cockades of typical sizes, as well as the physical

222 constraints on maximum flow rates in hydrothermal systems. As an example, we will consider an
223 aqueous fluid at 150°C with a salinity of 20 wt.% NaCl (3.4 mol/kg). This salinity is fairly high
224 (Roedder, 1984; Shepherd et al., 1985), resulting in comparatively high density and viscosity. Based
225 on the relations presented by Haas (1970), Kestin et al. (1978) and Mao and Duan (2009), this fluid
226 would have a density of 1.0 g/cm³, and a viscosity of 4.0 mPas. The flow threshold for fluidisation
227 of a loosely packed granular aggregate (voidage = 0.5) of quartz or calcite ($\rho = 2.7 \text{ g/cm}^3$) pebbles
228 with an equivalent hydraulic diameter of 5 cm (a fairly typical size for cockades, e.g. Leroy et al.,
229 2000), can be estimated from the relations given by Eichhubl and Boles (2000) to be 0.24 m/s. This
230 velocity value is reasonably robust against changes in salinity or temperature of the fluid, and
231 represents the absolute minimum for fluidisation to occur.

232 On the other hand, the minimum flow speeds needed for suspension of clasts in the fluid are
233 equal to their terminal settling velocity. The relevant relations for cube-shaped particles are given by
234 Gaskell (1992) and Pettyjohn and Christiansen (1948), and the result for the case described above is
235 0.88 m/s. Minimum fluid ascent velocities on the order of 10⁻¹ to 10⁰ m/s are therefore necessary, if
236 the formation of cockade breccias is to be explained by bed fluidisation or suspension.

237 The critical question is now whether such high flow velocities can be attained and also *sustained*
238 in fault-related hydrothermal systems. Unfortunately, there is virtually no data on fluid flow
239 velocities in terrestrial systems and no easy way to infer them from field evidence. Eichhubl and
240 Boles (2000) used fluid inclusion thermometry and oxygen isotope data to assess the temperature
241 anomaly associated with a carbonate vein along a strike-slip fault in California, which in turn
242 yielded an estimate of upward fluid flow velocities in the fault. Due to parameter uncertainties, they
243 arrived at a wide range of 10⁻⁴ to 10⁰ m/s for the velocity of *pulses* of hot fluid moving up the fault
244 (Eichhubl and Boles, 2000). This just includes the required minimum velocities calculated above,
245 but represents episodic and not sustained flow. Fluid flow in natural fault-related hydrothermal
246 systems is probably intermittent, due to the operation of seal-fracture and fault-valve processes
247 linked to seismic activity (Sibson, 1981; Cathles and Smith, 1983; Sibson et al., 1988; Boullier and
248 Robert, 1992; Eichhubl and Boles, 2000). Release of fluids from over-pressured reservoirs is
249 thought to be triggered when fluid pressures approach lithostatic pressure (Sibson, 1990). Thus the
250 maximum pressure gradient along a fault discharging fluids will be given by the difference between
251 the lithostatic and hydrostatic pressure gradients. If the shape of the fault conduit and the fluid
252 properties are known, the maximum (transient) flow velocity can be estimated. Approximating a
253 typical cockade-bearing fault cavity by a conduit with a rectangular cross section 100 m long and
254 0.5 m wide, using the same fluid as above (aqueous solution of NaCl, 20 wt.%, at 150°C), and
255 assuming the relative roughness of the fault walls to be on the order of 0.1 (i.e. that the short-
256 wavelength deviations of the fault walls from flat surfaces amount to about 10% of the total width

257 of the conduit), we arrive at a maximum velocity of ~ 20 m/s using the Darcy-Weisbach equation
258 (assuming an average rock density of 3.0 g/cm^3 ; De Nevers, 1970). This value is well above the
259 minimum requirement for clast fluidisation or suspension derived above. Consequently, this
260 mechanism cannot be ruled out as the driver for cockade rotation. However, it will probably only
261 occur for short periods of time when flow velocities peak due to the release of over-pressured fluids
262 during seismic events. The calculation of maximum flow rate assumes that the fault is fed by a
263 reservoir with no internal flow resistance, and discharges into a similar reservoir. Actual maximum
264 flow rates will probably be lower because the fluid reservoirs in natural systems are typically
265 porous rocks with a much lower permeability than large open fractures. Another consequence is that
266 high flow rates are probably not sustainable over extended periods of time. Measurements of natural
267 fluid flow velocities have been made at black smokers, where fluids have steady state exit velocities
268 of $0.5 - 5$ m/s (RISE, 1980; Macdonald et al., 1980; Converse et al., 1984; Hekinian et al., 1983,
269 1984). However, these high velocities are probably due to highly focussed flow at the exiting point
270 (cf. Strens and Cann, 1986), with each black smoker field fed by a large fracture network (Strens
271 and Cann, 1986). The high thermal gradients present around the centres of mid-ocean ridges may
272 also contribute to these high flow velocities. Additionally, mass flow rates of black smoker fields
273 are typically small compared to the expected discharge rate of the fault zone in our model
274 calculation. For fluid velocities of 0.2 to 0.9 m/s, a fault fracture 100 m long and 0.5 m wide would
275 discharge 10 to $45 \text{ m}^3/\text{s}$, while a black smoker field typically only discharges 150 kg/s of fluid
276 (Hekinian et al., 1984). Consequently, steady-state fluid flow velocities in the fracture system
277 associated with a black smoker field must be much smaller than the discharge velocities cited
278 above. Another argument for low steady-state flow velocities is the significantly smaller pressure
279 gradient resulting from temperature induced density differences, compared to the maximum
280 pressure gradient assumed above.

281 It is clear from the foregoing discussion that *intermittent* fluidisation and cementation of clasts
282 cannot be ruled out as a mechanism for the formation of cockade breccias. However, the
283 calculations indicate that *sustained* suspension of cockades over extended periods of time is highly
284 unlikely: the required flow velocities and volume flow rates would be too large. Sustained
285 suspension (or fluidisation) and simultaneous cementation in a rapidly ascending low-viscosity
286 aqueous fluid can therefore be discounted as a realistic formation mechanism for cockade breccias.

287

288 4.4. Rotation-accretion hypothesis

289 Intermittent fluidisation or suspension and subsequent partial cementation essentially describe the
290 rotation-accretion mechanism (6). The hypothesis specifies no specific mechanism for the re-
291 fracturing of the partially cemented breccia and the subsequent rotation of clasts. However, the re-

292 fracturing that would have to precede re-suspension or re-fluidisation can probably only be
293 achieved by the mechanical action of moving fault walls and not the moving fluid alone.
294 Cementation is expected to occur mostly in interseismic periods (cf. Eichhubl and Boles, 2000), and
295 significantly higher flow rates would be required to dislodge partially cemented clasts than to
296 fluidise or suspend non-cemented ones.

297 Identification of the primary driver for clast agitation might be possible from textural
298 relationships, specifically grading relations. While a cockade breccia unit formed from fluidisation
299 of individual cockades would be expected to show normal grading of cockade sizes, due to the
300 faster settling velocities of larger particles, one formed primarily through the action of fault wall
301 movement and associated agitation (shaking) without fluidisation should show reverse grading
302 because of the Brazil-nut effect, that is, the tendency of larger particles in an agitated self-
303 supporting mass of non-equigranular particles to migrate towards the top (Möbius et al., 2001). The
304 frustrating result this effect can have on the distribution of nuts and dried fruit in packages of
305 breakfast cereal should be familiar to most readers. In the only case of cockades where grading
306 relationships have actually been reported, reverse grading is observed (Genna et al., 1996),
307 indicating the dominance of seismic shaking or fault shear for the re-fracturing and rotation of the
308 breccia unit.

309

310 *4.5. Other hypotheses*

311 Replacement processes (4) will result in their own characteristic set of textures which are easily
312 distinguishable from the space-filling growth of minerals (Bastin, 1950), while the infall of clasts
313 during cementation (5) would not yield cement crusts completely enclosing the fragments and
314 would result in a distinctive asymmetric overall texture (Fig. 1e) which is not usually observed.

315 Considering the evidence available from the literature, the rotation-accretion mechanism of
316 formation (6), the textural implications of which are discussed in section 5, may be regarded as
317 being the most likely to explain all of the observed features, although different mechanisms might
318 be responsible for the necessary re-fracturing and rotation. Replacement processes might contribute
319 to the formation of some cockade-like textures.

320

321 **5. Textural evidence for the rotation-accretion mechanism of cockade breccia formation**

322

323 If repeated rotation and accretion is the most likely mechanism for the formation of cockade
324 breccias, the following textures would be expected on the macro- to microscale:

325

326 1) Open space-filling cement textures, e.g. colloform or columnar growths, well-developed

- 327 crystal faces;
- 328 2) Lack of contact-points between clasts in 3D;
 - 329 3) Lack of extensive replacements;
 - 330 4) Points of breakage or missing sections in the cement layers where clasts formerly touched
 - 331 each other and thus hindered the development of complete encrustations;
 - 332 5) Rotated geopetal ('way up') indicators, such as sediment deposited on and around the clasts.
- 333

334 In addition to these essential textures, the following are expected to be developed depending on the
335 primary driver for breccia re-fracturing and clast rotation:

336

- 337 6) Reverse grading of cockades within individual breccia units – resulting from the Brazil Nut
 - 338 or Muesli Effect in an agitated non-equigranular material (Möbius et al., 2001), which might
 - 339 be accompanied by an upward-increasing cement to clasts ratio. This will result if seismic
 - 340 shaking is the dominant mechanism for re-fracturing of the breccia and rotation of clasts.
 - 341 7) Normal grading of cockades within individual breccia units – resulting from the faster
 - 342 settling velocities of larger clasts, if intermittent fluidisation or suspension is the dominant
 - 343 mechanism for re-fracturing and rotation of clasts.
- 344

345 The most thorough study of rotation-accretion cockade breccias (Genna et al., 1996) detailed
346 only the reverse grading of cockades (6) and mentioned their mechanical attrition (4). Van Alstine
347 (1944) described evidence that clasts do not touch in 3D (2). Neither study involved detailed
348 microscopic analyses of the textures. The necessity for a more comprehensive study of well-
349 exposed cockade breccias is indicated by this lack of published data. Material found by the authors
350 during an investigation of low-temperature, near-surface veins on the Gower peninsula, South
351 Wales, will serve to illustrate a few more of the textural aspects described above.

352

353 **6. Geological setting of Gower veins, Gower peninsula, Wales**

354

355 Abundant calcite-haematite veins outcrop within the Pembroke Limestone Group (Mississippian,
356 lower Carboniferous) along the southern coast of the Gower Peninsula, South Wales (Fig. 2a). They
357 occur along dilational strike-slip faults active late in the tectonic history of the Gower (George,
358 1940; Roberts, 1979), towards the end of the Variscan orogeny (Wright et al. 2009) and probably
359 during Mesozoic rifting of the Bristol Channel Basin (Woodcock et al., in press; Ault, personal
360 communication). Wright et al. (2009) documented a range of syndeformational open-void filling
361 textures including the occurrence of cockade breccias. Formerly economic haematite mineralisation

362 is present in some veins and might be related to the iron deposits of the Taff's Well/Llanharry ore
363 field east of Swansea. The general nature of the fills, their simple mineralogy, and similarity to other
364 deposits for which reasonable temperature constraints can be given (Dunham, 1984; Rankin and
365 Criddle, 1985) indicates that formation probably occurred below 150°C.

366 Material for the present study was collected from the central part of the eastern vein at Oxwich
367 (Fig. 8a of Wright et al., 2009). Cockades only make up a small part of the East Oxwich vein,
368 occurring as the latest fill in a 20 to 50 cm wide zone cutting across the boundaries of all previous
369 fills (Fig. 2b). They range from about 2 – 10 cm in diameter and consist almost entirely of several
370 generations of columnar ferroan calcite cement, overgrowing clasts of previous calcite vein fills or
371 of limestone. Later alteration processes including the partial leaching of ferrous iron from the
372 calcite, oxidation and precipitation of finely disseminated ferric hydroxide caused the orange-brown
373 colour of the haematite-free calcite now observed in the outcrop.

374

375 **7. Textural evidence from the Gower cockades**

376

377 While much of the cockade breccia unit is massive, some parts still show remnant porosity (Fig.
378 3). Sampling was from one of these parts, and was aided by the fact that individual cockades tended
379 to break off along the sutures between the last generation of cement growing on adjacent clasts.
380 This also demonstrated the lack of contact-points between clasts – individual fragments were found
381 to be completely and evenly surrounded by cement on all sides. This was confirmed by the
382 preparation of serial horizontal sections cut from several cockades. Figures 4 and 5 show detailed
383 line drawings and the corresponding photographs of three parallel sections through one of the larger
384 examples. The central sparry calcite clast is evidently not supported by other clasts on its lower
385 side, parts of which would be expected to be seen in the last section.

386 The cement itself is exclusively columnar to blocky, with most individual crystals showing well-
387 developed growth faces. These are picked out by layers of fine-grained haematite inclusions which
388 appear to have coated the cockade at irregular intervals during its formation. The haematitic
389 material probably originated from the comminution of massive haematite during fault movements
390 within higher parts of the vein or as a direct precipitate from the solutions, and behaves as an
391 internal sediment. This behaviour is illustrated by its tendency to coat individual calcite crystals
392 only on their upward pointing faces in other parts of the vein system (Fig. 6a), as well as forming
393 characteristic drapings which are thinnest at the tips of the crystals and become thicker in the spaces
394 between crystals (Fig 6b). Such differences in thickness are only expected from sedimentation. A
395 third characteristic illustrating the primarily sedimentary nature of the haematite coatings is the
396 embedding of some larger fragments (up to a few millimetres in size) in these layers (Fig. 6c).

397 Finally, similar material present in other parts of the vein shows normal grading (Fig. 6d). Notably,
398 the thickest layers of the haematitic sediment occur towards different sides of the cockades within
399 different cement generations, and sometimes even on what is now the lower surface of the central
400 clast (Figs. 4 and 5). It can also be seen from Fig. 4 that breakage points are occasionally present
401 within the haematite and cement layers. Similar textures are present in all of the material collected.

402 The five essential textural characteristics expected for cockades formed by the rotation-accretion
403 mechanism (see above) are therefore met by the Gower material. Unfortunately, the extent of the
404 cockade breccia unit and the nature of the exposure (horizontal section) did not allow for the
405 observation of any grading relationships and the dominant agitation mechanism could therefore not
406 be assessed. The sedimentary behaviour of the very fine-grained haematitic material indicates that
407 maximum fluid velocities must have been very low during the formation and subsequent
408 cementation of the haematitic layers. Obviously, a fluid velocity in which material with an average
409 grain size of $< 100 \mu\text{m}$ can settle is much too low to fluidise much coarser material (cm-sized
410 cockades), though the intermittent occurrence of high-flow events cannot be ruled out. Intervals
411 evidently occurred in which no sedimentation of haematitic material took place (Figs. 4 and 5). If
412 high-velocity flow did occur, it must have alternated with periods of low-velocity flow. It is difficult
413 to assess the exact number of rotation and accretion cycles which occurred during the formation of
414 the Gower cockades, since this would require the identification of all or most breakage points in the
415 cement layers surrounding the cockades. However, from the points identifiable in the sections
416 shown, there must have been at least two events after the initial formation of the central clast. If the
417 occurrence of the thick layers of haematitic sediment is related to individual slip events, then at
418 least four such events can be counted.

419 In conclusion, the evidence from the Gower strongly supports the rotation-accretion mechanism
420 for cockade breccia formation as envisaged by Van Alstine (1944) and to an extent Genna et al.
421 (1996). Although the dominant agitation mechanism (fault wall movement or high-flow events)
422 could not be assessed, the above description considerably complements their observations.

423

424 **8. Cockade breccias as indicators for relative cementation rates**

425

426 Persistent void space between cockades throughout their formation is evidenced by a) the rarity
427 of contact points, b) the abundance of nicely developed calcite crystal terminations (Fig. 4), and c)
428 the incomplete infill between cockades at the present outcrop (Fig. 3). Similar observations were
429 made by Genna et al. (1996) on the cockade breccias in the Cirotan gold mine, Indonesia.
430 Incomplete cementation between bursts of tectonic activity is probably one of the key requirements
431 for the formation of cockade textures, since it allows for relatively easy breakage along the

432 cemented sutures between adjacent cockades. Such fracture sites in turn ensure that individual
433 cockades remain mostly intact through each fracturing event and can slowly accumulate their
434 successive cement coatings (Fig. 7a). This tendency to break between rather than across clasts was
435 observed during sampling, particularly in the poorly cemented parts of the unit, supporting the
436 notion that it also occurred during fault displacement. If cementation had been complete before
437 every fault-slip episode, specific points of weakness would have been lacking. Fracture would have
438 occurred across clasts, resulting in different generations of cross-cutting fracture fills (Fig. 7b).

439 Since fracturing by either movement of the fault walls or rapidly ascending fluids will always be
440 related to fault slip (as discussed earlier) it is proposed that cockade breccias form along dilational
441 faults where the rate of hydrothermal cementation is slow compared to the rate of fault slip. An
442 abundance of cockades relative to other kinds of breccia vein fills therefore provides a proxy for
443 either low cementation rate or high fault slip rate. In Gower, the abundance of cockade breccias is
444 relatively low compared to other types of breccia, while in the Cirotan gold-mine it appears to be
445 relatively high (Genna et al., 1996). However, calibrating absolute rates of either cementation or
446 fault-slip on ancient faults remains problematic.

447 448 **9. Random packing of granular materials and (cockade) breccia classification**

449
450 There is a nomenclatural problem with many cockade breccias: the ratio of original clasts to
451 crystalline cement is generally so low ($< 30\%$, cf. Table 2) that they would be classified as ‘vein
452 fills’ rather than ‘breccia’ on the scheme of Woodcock and Mort (2008, Fig. 5b). This section
453 addresses this issue.

454 Random packing of similarly sized grains of different shapes results in maximum porosities of
455 about 50 % (Wyllie and Gregory, 1953). Random packing of non-equigranular materials results in
456 lower porosity, because spaces between the larger grains are filled by some of the smaller grains.
457 Therefore, in a cement-rich breccia resulting from a single fracturing event followed by
458 cementation, the percentage of clasts should not be less than 50 %, well above the 30% threshold
459 chosen by Woodcock and Mort (2008). However, where fragmentation results in a high proportion
460 of small clasts (< 2 mm, Woodcock and Mort, 2008) and matrix (< 0.1 mm), the proportion of large
461 clasts in fault rocks is commonly lower than 30 %, beyond which threshold the rocks are classified
462 as cataclasites or mylonites (Woodcock and Mort, 2008, Fig. 5b).

463 Table 2 shows the proportion of cement (and minor matrix) present in photographs of seven
464 published occurrences of cockade breccias. These examples mostly have negligible fine-grained
465 matrix but an average of over 70 % cement. Clearly, clasts in these breccias cannot and do not form
466 a self-supporting framework. It also means that many cockade breccias are not strictly breccias

467 according to Figure 5b of Woodcock and Mort (2008). They have less than 30 % large clasts, and
468 therefore classify as vein-fills.

469 The genetic explanation for the difficulty in classifying cockade breccias lies in their formation
470 by repeated fracturing and cementation events. Mechanically, the ‘clasts’ produced by later
471 fracturing events are composites of the original clasts and the early cement. Having recognised this
472 nomenclatural difficulty, we do not propose to pursue it. There are many geometric problems in
473 classifying the spectrum from vein-fills to cement-rich breccias, which lie beyond the scope of this
474 paper. Whilst the purist may want to use the term *cockade texture* for examples with a low clast
475 percentage, we suggest that *cockade breccia* is a pragmatic choice unlikely to be misunderstood.

476

477 **10. Correct identification of cockade breccias**

478

479 Criteria are listed below to help in the correct identification of proper cockade breccias,
480 particularly in the field. The following five criteria should be observable in any cockade breccia
481 (also see Fig. 8):

482

- 483 1) Concentric banding around clasts,
- 484 2) Columnar cement and, or, other space-filling textures;
- 485 3) Sharp boundaries between clasts and the first cement generation (i.e. no evidence for
486 replacement, although this might not be detectable on the macro-scale);
- 487 4) Volume proportion of cement significantly higher than 50%;
- 488 5) Clasts not touching. This might be demonstrated either by extracting single cockades from
489 the outcrop (such as was done for this work) or by serial sectioning of samples containing at
490 least one or two whole clasts.

491

492 Two further criteria might be evident from lab-based investigations:

493

- 494 6) Points of breakage in cement layers where cockades were previously touching each other;
- 495 7) Rotated geopetal indicators (such as the haematitic sediment in the present case).

496

497 Of particular significance, especially for the distinction between cockade breccias and single-
498 phase breccias cemented by multiple cement generations are criteria (4) to (7). The volume
499 proportion (4) provides the strongest clue, and should be observable in the field. It should also be
500 preserved if later overprinting or alteration of the breccia has removed some or most of the other
501 textural evidence such as columnar cement textures (2) or clast/cement contacts (3).

502 Two different mechanisms are expected to contribute to the mechanical agitation necessary for
503 cockade formation: fault wall movement and fault slip-induced rapid fluid flow. If cockade breccia
504 units are of a sufficient size to show grading relationships, the dominant agitation mechanism might
505 be identified. In particular, reverse grading is expected if fault wall movement was dominant, while
506 normal grading is expected if a rapidly ascending fluid was dominant.

507 It will be noted that the criteria given above specifically limit the definition of the term *cockade*
508 *breccia* to those structures formed by the rotation-accretion mechanism. For the superficially similar
509 structures formed by partial metasomatic replacement of clast minerals, a different term should be
510 used. The genetic implications of their occurrence are quite different to that of cockade breccias.

511

512 11. Conclusions

513

- 514 • Cockade textures have been recognised in mineral veins since 1836, with the term *cockade*
515 being used since 1859 for concentric banding of mineral cements around breccia clasts.
- 516 • A review of 106 published descriptions of cockade breccias shows that about half of the
517 examples come from epithermal Au-(Ag, Cu) veins, a quarter from mainly epithermal Pb-
518 Zn-(Cu, Ag, Sn) veins, and the remainder from other parageneses.
- 519 • At least six mechanisms have been proposed for the formation of cockade breccia-like
520 textures, but only two – repeated rotation-accretion, and partial metasomatic replacement of
521 clast minerals – have been supported by detailed evidence.
- 522 • A new example of cockade breccia, from the East Oxwich fault on the Gower Peninsula
523 (South Wales), shows clear evidence for the rotation-accretion mechanism, particularly
524 overgrown breakage points in cement layers, where cockades were previously touching each
525 other, and rotated geopetal infills of hematitic sediment.
- 526 • Cockade textures probably result from low rates of cement growth compared to high rates of
527 dilational fault slip. Seven criteria are given for the correct identification of cockade breccia.
- 528 • Grading relationships can be used to identify the driver mechanism for re-fracturing and
529 cockade rotation. This is relevant since such cases where rapid fluid flow can be
530 demonstrated to have been the dominant driver mechanism might be used to constrain
531 maximum fluid flow velocities.
- 532 • Due to their different genetic implications, cockade breccia-like textures resulting from
533 partial metasomatic replacement of clast minerals should not be called cockade breccias.
534 The criteria defined above may be used to distinguish them from cockade breccias *sensu*
535 *stricto*.

536

537 **Acknowledgements**

538

539 Many thanks are due to Tobias Fusswinkel and Atsushi Okamoto for their constructive comments
540 which helped to significantly improve this article, while Martin Walker is thanked for help with the
541 preparation of thin sections, and Sarah Humbert for providing moral guidance and being a most
542 excellent librarian.

543

544 **References**

545

546 Bastin, E.S., 1925. Primary native silver ores of South Lorraine and Cobalt, Ontario. *Economic*
547 *Geology* 20, 1–24.

548 Bastin, E.S., 1950. Interpretation of ore textures. Geological Society of America, Washington, D.C.

549 Bateman, A.M., 1924. Angular inclusions and replacement deposits. *Economic Geology* 19, 504–
550 520.

551 Beck, R., 1903. *Lehre von den Erzlagerstätten*. 2nd Ed., Gebrüder Bornträger, Berlin.

552 Bélistont, R., Boiron, M.-C., Luais, B., Cathelineau, M., 2014. LA-ICP-MS analyses of minor and
553 trace elements and bulk Ge isotopes in zoned Ge-rich sphalerites from the Noailhac – Saint-
554 Salvy deposit (France): insights into incorporation mechanisms and ore deposition
555 processes. *Geochimica et Cosmochimica Acta* 126, 518–540.

556 Boriani, A., Burlini, L., Caironi, V., Origoni, E.G., Sassi, A., Sesana, E., 1988. Geological and
557 petrological studies on the hercynian plutonism of Serie dei Laghi – geological map of its
558 occurrence between Valsesia and Lago Maggiore (N-Italy). *Rendiconti della Società Italiana*
559 *di Mineralogia e Petrologia* 43, 367–384.

560 Boullier, A.-M., Robert, F., 1992. Palaeoseismic events recorded in Archaean gold-quartz vein
561 networks, Val d'Or, Abitibi, Quebec, Canada. *Journal of Structural Geology* 14, 161–179.

562 Buerger, M.J., Maury, J.L., 1927. The ores of Chocaya, Bolivia. *Economic Geology* 22, 1–13.

563 Byrne, D.R., Harris, L.B., 1993. Structural controls on the base-metal vein deposits of the
564 Northampton Complex, Western Australia. *Ore Geology Reviews* 8, 89–115.

565 Caine, J.S., Evans, J.P. Forster, C.B. 1996. Fault zone architecture and permeability structure.
566 *Geology* 24, 1025–1028.

567 Cathles, L.M., Smith, A.T., 1983. Thermal constraints on the formation of Mississippi Valley-type
568 lead-zinc deposits and their implications for episodic basin dewatering and deposit genesis.
569 *Economic Geology* 78, 983–1002.

570 Clar, E., 1929. Über die Blei-Zinklagerstätte St. Veit bei Imst (Nordtirol). *Jahrbuch der*
571 *Geologischen Bundesanstalt* 79, 333–356.

- 572 Converse, D.R., Holland, H.D., Edmond, J.M., 1984. Flow rates in the axial hot springs of the East
573 Pacific Rise (21°N): implications for the heat budget and the formation of massive sulphide
574 deposits. *Earth and Planetary Science Letters* 69, 159–175.
- 575 Cotta, B., 1859. *Lehre von den Erzlagerstätten*. J.G. Engelhardt, Freiberg.
- 576 Cotta, B., 1870. *A treatise on ore deposits*. Translation of 2nd German Ed. by Prime, F., Van
577 Nostrand, New York.
- 578 De Nevers, 1970. *Fluid Mechanics*. Addison-Wesley, Reading, Massachusetts.
- 579 Dill, H.G., Weber, B., 2010. Variation of color, structure and morphology of fluorite and the origin
580 of the hydrothermal F-Ba deposits at Nabburg-Wölsendorf, SE Germany. *Neues Jahrbuch
581 für Mineralogie – Abhandlungen* 187, 113–132.
- 582 Dunham, K.C., 1984. Genesis of the Cumbrian hematite deposits. *Proceedings of the Yorkshire
583 Geological Society* 45, 130
- 584 Eichhubl, P., Boles, J.R., 2000. Rates of fluid flow in fault systems – evidence for episodic rapid
585 fluid flow in the Miocene Monterey Formation, coastal California. *American Journal of
586 Science* 300, 571–600
- 587 Farmin, R., 1938. Dislocated inclusions in gold-quartz veins at Grass Valley, California. *Economic
588 Geology* 33, 579–599.
- 589 Faulkner, D.R., Jackson, C.A.L., Lunn, R.J., Schlische, R.W., Shipton, Z.K., Wibberley, C.A.J.,
590 Withjack, M.O., 2010. A review of recent developments concerning the structure, mechanics
591 and fluid flow properties of fault zones. *Journal of Structural Geology* 32, 1557–1575.
- 592 Feitinger, G., Paar, W.H., 1991. Gangförmige Gold-Silber-Vererzungen in der Sonnblickgruppe
593 (Hohe Tauern, Kärnten). *Archiv für Lagerstättenforschung der Geologischen Bundesanstalt
594* 13, 17–50.
- 595 Feitinger, G., Paar, W.H., Tarkian, M., Reche, R., Weinzierl, O., Prochaska, W., Holzer, H., 1995.
596 Vein type Ag-(Au)-Pb, Zn, Cu-(W,Sn) mineralization in the Southern Kreuzeck Mountains,
597 Carinthia Province, Austria. *Mineralogy and Petrology* 53, 307–332.
- 598 Fusswinkel, T., Wagner, T., Wenzel, T., Wälle, M., Lorenz, J., 2013. Evolution of unconformity-
599 related Mn – Fe – As vein mineralization, Sailauf (Germany): Insight from major and trace
600 elements in oxide and carbonate minerals. *Ore Geology Reviews* 50, 28–51.
- 601 Fusswinkel, T., Wagner, T., Wenzel, T., Wälle, M., Lorenz, J., 2014. Red bed and basement sourced
602 fluids recorded in hydrothermal Mn-Fe-As veins, Sailauf (Germany): A LA-ICPMS fluid
603 inclusion study. *Chemical Geology* 363, 22–39.
- 604 Gaskell, D.R., 1992. *An introduction to transport phenomena in materials engineering*. Macmillan,
605 New York.
- 606 Genkin, A.D., Bortnikov, N.S., Cabri, L.J., Wagner, F.E., Stanley, C.J., Safonov, Y.G., McMahon, G.,

- 607 Friedl, J., Kerzin, A.L., Gamyamin, G.N., 1998. A multidisciplinary study of invisible gold in
608 arsenopyrite from four mesothermal gold deposits in Siberia, Russian Federation. *Economic*
609 *Geology* 93, 463–487.
- 610 Genna, A., Jébrak, M., Marcoux, E., Milési, J.P., 1996. Genesis of cockade breccias in the tectonic
611 evolution of the Cirotan epithermal gold system, West Java. *Canadian Journal of Earth*
612 *Sciences* 33, 93–102.
- 613 George, T.N., 1940. The structure of Gower: *Quarterly Journal of the Geological Society of London*
614 96, 131–198.
- 615 Gibson, P.C., Noble, D.C., Larson, L.T., 1990. Multistage evolution of the Calera epithermal Ag-Au
616 vein system, Orcopampa District, southern Peru: First results. *Economic Geology* 85, 1504–
617 1519.
- 618 Grancea, L., Bailly, L., Leroy, J., Banks, D., Marcoux, E., Milési, J.P., Cuney, M., André A.S.,
619 Istvan, D., Fabre, C., 2002. Fluid evolution in the Baia Mare epithermal gold/polymetallic
620 district, Inner Carpathians, Romania. *Mineralium Deposita* 37, 630–647.
- 621 Haas, J.L., 1970. An equation for the density of vapor-saturated NaCl-H₂O solutions from 75° to
622 325°C. *American Journal of Science* 269, 489–493.
- 623 Hagemann, S.G., Groves, D.I., Ridley, J.R., Vearncombe, J.R., 1992. The Archean lode gold
624 deposits at Wiluna, Western Australia: High-level brittle-style mineralisation in a strike-slip
625 regime. *Economic Geology* 87, 1022–1053.
- 626 Hekinian, R., Francheteau, J., Renard, V., Ballard, R.D., Choukroune, P., Cheminée, J.L., Albarède,
627 F., Minster, J.F., Marty, J.C., Boulegue, J., Charlou, J.L., 1983. Intense hydrothermal activity
628 at the axis of the East Pacific Rise near 13°N: submersible witnesses the growth of sulphide
629 chimney. *Marine Geophysical Research* 6, 1–14.
- 630 Hekinian, R., Renard, V., Cheminée, J.L., 1984. Hydrothermal deposits on the East Pacific Rise
631 near 13°N: geological setting and distribution of active sulfide chimneys. In: Rona, P.A.,
632 Bostrom, K., Laubier, L., Smith, K.L. (Eds.), *Hydrothermal Processes at Seafloor Spreading*
633 *Centers*. Plenum, New York, 571 – 594.
- 634 Hilgers, C., Urai J.L., 2005. On the arrangement of solid inclusions in fibrous veins and the role of
635 the crack-seal mechanism. *Journal of Structural Geology* 27, 481–494.
- 636 Hodgson, C.J., 1989. The structure of shear-related, vein-type gold deposits: a review. *Ore Geology*
637 *Reviews* 4, 231–273.
- 638 Ilavský, J., Turan, J., Turanová, 1991. Magnesite deposits and occurrences in the West Carpathians
639 of Czecho-Slovakia. *Ore Geology Reviews* 6, 537–561.
- 640 Ingham, A.I., 1940. The zinc and lead deposits of Shawangunk Mountain, New York. *Economic*
641 *Geology* 35, 751–760.

- 642 Jicha, H.L., 1951. Alpine lead-zinc ores of Europe. *Economic Geology* 46, 707–730.
- 643 Jobson, D.H., Boulter, C.A., Foster, R.P., 1994. Structural controls and genesis of epithermal gold-
644 bearing breccias at the Lebong Tandai mine, Western Sumatra, Indonesia. *Journal of*
645 *Geochemical Exploration* 50, 409–428.
- 646 Kalliokoski, J., 1965. Metamorphic features in North American massive sulfide deposits. *Economic*
647 *Geology* 60, 485–505.
- 648 Kestin, J., Sokolov, M., Wakeham, W.A., 1978. Viscosity of liquid water in the range -8°C to
649 150°C. *Journal of Physical and Chemical Reference Data* 7, 941–948.
- 650 Kontak, D.J., Ansdell, K., Archibald, D., 1999. New constraints on the age and origin of the
651 Dunbrack Pb-Cu-Zn-Ag deposit, Musquodoboit batholith, southern Nova Scotia. *Atlantic*
652 *Geology* 35, 19–42.
- 653 Kucha, H., Van der Biest, J., Viaene, W.A., 1990. Peloids in stratabound Zn-Pb deposits and their
654 genetic importance. *Mineralium Deposita* 25, 132–139.
- 655 Kutina, J., Sedlackova, J., 1961. The role of replacement in the origin of some cockade textures.
656 *Economic Geology* 56, 149–176.
- 657 Laznicka, P., 1988. Breccias and coarse fragmentites: petrology, environments, associations, ores.
658 *Developments in Economic Geology* 25, Elsevier, Amsterdam.
- 659 Leroy, Jacques L., Hubé, Daniel, Marcoux, E., 2000. Episodic deposition of Mn-minerals in
660 cockade breccia structures in three low-sulfidation epithermal deposits: a mineral
661 stratigraphy and fluid inclusion approach. *The Canadian Mineralogist* 38, 1125–1136.
- 662 Lindgren, W., 1919. *Mineral Deposits*. 2nd ed., McGraw-Hill, New York.
- 663 Liu, Y., Chi, G., Bethune, K.M., Dubé, B., 2011. Fluid dynamics and fluid-structural relationships in
664 the Red Lake mine trend, Red Lake greenstone belt, Ontario, Canada. *Geofluids* 11, 260–
665 279.
- 666 Macdonald, K.C., Becker, K., Spiess, F.N., Ballard, R.D., 1980. Hydrothermal heat flux of the
667 „black smoker“ vents on the East Pacific Rise. *Earth and Planetary Science Letters* 48, 1–7.
- 668 Mao, S., Duan, Z., 2009. The viscosity of aqueous alkali-chloride solutions up to 623 K, 1,000 bar,
669 and high ionic strength. *International Journal of Thermophysics* 30, 1510 – 1523
- 670 Möbius, M.E., Lauderdale, B.E., Nagel, S.R., Jaeger, H.M., 2001. Brazil-nut effect: Size separation
671 of granular particles. *Nature* 414, 270.
- 672 Mort, K., Woodcock, N.H., 2008. Quantifying fault breccia geometry: Dent Fault, NW England.
673 *Journal of Structural Geology* 30, 701–709.
- 674 Munoz, M., Boyce, A.J., Courjault-Rade, P., Fallick, A.E., Tollon, F., 1994. Multi-stage fluid
675 incursion in the Palaeozoic basement-hosted Saint-Salvy ore deposit (NW Montagne Noire,
676 southern France). *Applied Geochemistry* 9, 609–626.

- 677 Munoz, M., Boyce, A.J., Courjault-Rade, P., Fallick, A.E., Tollon, F., 1999. Continental basinal
678 origin of ore fluids from southwestern Massif Central fluorite veins (Albigeois, France):
679 evidence from fluid inclusion and stable isotope analyses. *Applied Geochemistry* 14, 447–
680 458.
- 681 Noriel, C., Renard, F., Doan, M.-L., Gratier, J.-P., 2010. Intense fracturing and fracture sealing
682 induced by mineral growth in porous rocks. *Chemical Geology* 269, 197–209.
- 683 Okrusch, M., Lorenz, J.A., Weyer, S., 2007. The genesis of sulfide assemblages in the former
684 Wilhelmine mine, Spessart, Bavaria, Germany. *The Canadian Mineralogist* 45, 723–750.
- 685 Patrier, P., Bruzac, S., Pays, R., Beaufort, D., Bouchot, V., Verati, C., Gadalia, A., 2013. Occurrence
686 of K-feldspar-bearing hydrothermal breccias in the Bouillante geothermal field (Basse
687 Terre–Guadeloupe). *Bulletin de la Societe geologique de France* 184, 119–128.
- 688 Penczak, R.S., Mason, R., 1997. Metamorphosed Archean epithermal Au-Sb-Zn(Hg) vein
689 mineralisation at the Campbell Mine, Northwestern Ontario. *Economic Geology* 92, 696–
690 719.
- 691 Perelló, J.A., 1994. Geology, porphyry Cu-Au, and epithermal Cu-Au-Ag mineralisation of the
692 Tombulilato district, North Sulawesi, Indonesia. *Journal of Geochemical Exploration* 50,
693 221–256.
- 694 Pettyjohn, E.S., Christiansen, E.B., 1948. Effect of particle shape on free-settling rates of isometric
695 particles. *Chemical Engineering Progress* 44, 157–172
- 696 Philipp, S.L., 2008. Geometry and formation of gypsum veins in mudstones at Watchet, Somerset,
697 SW England. *Geological Magazine* 145, 831–844.
- 698 Pošepný, F., 1895. The genesis of ore deposits. American Institute of Mining Engineers, New York.
- 699 Rankin, A.H., Criddle, A.J. 1985. Mineralizing fluids and metastable low temperature inclusion
700 brines at Llanharry iron deposit, South Wales. *Transactions of the Institution of Mining and*
701 *Metallurgy, Section B: Applied Earth Science* 94, 126–132.
- 702 Rieder, M., 1969. Replacement and cockade textures. *Economic Geology* 64, 564–567.
- 703 RISE, 1980. Hot springs and geophysical experiments on the East Pacific Rise. *Science* 207, 1421–
704 1433.
- 705 Roberts, J.C., 1979. Jointing and minor tectonics of the South Gower Peninsula between Mumbles
706 Head and Rhossili Bay, South Wales. *Geological Journal* 14, 1–14.
- 707 Roedder, E., 1984. Fluid inclusions: an introduction to studies of all types of fluid inclusions, gas,
708 liquid, or melt, trapped in materials from earth and space, and their application to the
709 understanding of geologic processes. *Reviews in Mineralogy, Mineralogical Society of*
710 *America, Blacksburg.*
- 711 Schneider, J., Boni, M., Laponi, F., 2002. Carbonate-hosted zinc-lead deposits in the Lower

- 712 Cambrian of Hunan, South China: A radiogenic (Pb, Sr) isotope study. *Economic Geology*
713 97, 1815–1827.
- 714 Shepherd, T.J., Rankin, A.H., Alderton, D.H.M., 1985. A practical guide to fluid inclusion studies.
715 Blackie & Son Ltd., Glasgow and London.
- 716 Sibson, R.H., 1981. Fluid flow accompanying faulting: field evidence and models. In: Simpson,
717 D.W., Richards, P.G. (Eds.), *Earthquake prediction: An international review*. American
718 Geophysical Union, Maurice Ewing Series 4, 897–900.
- 719 Sibson, R.H., 1990. Conditions for fault-valve behaviour. *London Geological Society Special*
720 *Publication* 54, 15–28.
- 721 Sibson, R.H., Robert, F., Poulsen, K.H., 1988. High-angle reverse faults, fluid-pressure cycling, and
722 mesothermal gold-quartz deposits. *Geology* 16, 551–555.
- 723 Sperling, H., 1973. Die Erzgänge des Erzbergwerks Grund (Silbernaaler Gangzug,
724 Bergwerksglucker Gang und Laubhütter Gang). *Monographien der deutschen Blei-Zink*
725 *Erzlagerstätten* 3 H.2, Geologisches Jahrbuch D, Schweizerbart, Stuttgart.
- 726 Spurr, J.E., 1926. Successive banding around rock fragments in veins. *Economic Geology* 21, 519–
727 537.
- 728 Squires, G.C., 2005. Gold and antimony occurrences of the Exploits subzone and Gander zone: a
729 review of recent discoveries and their interpretation. Newfoundland and Labrador
730 Department of Natural Resources Geological Survey Report 05-1, 223–237.
- 731 Strens, M.R., Cann, J.R., 1986. A fracture loop thermal balance model of black smoker circulation.
732 *Tectonophysics* 122, 307–324.
- 733 Suh, C.E., Dada, S.S., 1997. Fault rocks and differential reactivity of minerals in the Kanawa
734 Violaine uraniferous vein, NE Nigeria. *Journal of Structural Geology* 19, 1037–1044.
- 735 Taber, S., 1918. The mechanics of vein formation. *Transactions of the American Institute of Mining*
736 *Engineers* 140, 1189–1222.
- 737 Talmage, S.B., 1929. The significance of “unsupported” inclusions. *Economic Geology* 24, 601–
738 610.
- 739 Van Alstine, R.E., 1944. The fluorspar deposits of St. Lawrence, Newfoundland. *Economic Geology*
740 39, 109–132.
- 741 Vishiti, A., Petersen, S., Suh, C.E., Devey, C.W., 2013. Texture, mineralogy and geochemistry of
742 hydrothermally altered submarine volcanics recovered southeast of Cheshire Seamount,
743 western Woodlark Basin. *Marine Geology* (in press,
744 <http://dx.doi.org/10.1016/j.margeo.2013.11.002>)
- 745 Watson, K.D.P., 1943. Colloform sulphide veins of Port au Port peninsula, Newfoundland.
746 *Economic Geology* 38, 621–647.

- 747 Weissenbach, C.G.A., 1836. Abbildungen merkwürdiger Gangverhältnisse aus dem sächsischen
748 Erzgebirge. Leopold Voss, Leipzig.
- 749 Wiltschko, D.V., Morse, J.W., 2001. Crystallization pressure versus “crack seal” as the mechanism
750 for banded veins. *Geology* 29, 79–82.
- 751 Woodcock, N.H., Miller, A.V.M., Woodhouse, C.D., in press. Chaotic breccia zones on the
752 Pembroke Peninsula, South Wales: collapse into voids along dilational faults. *Journal of*
753 *Structural Geology*.
- 754 Woodcock, N.H., Dickson, J.A.D., Tarasewicz, J.P.T., 2007. Transient fracture permeability and
755 reseal hardening in fault zones: evidence from dilation breccia textures, in: Lonergan, L.,
756 Jolly, R.J.H., Rawnsley, K., Sanderson, D.J. (Eds.), *Fractured Reservoirs*, Geological
757 Society, London, Special Publication 270, 43–53.
- 758 Woodcock, N.H., Mort, K., 2008. Classification of fault breccias and related fault rocks. *Geological*
759 *Magazine* 145, 435–440.
- 760 Wright, V., Woodcock, N.H., Dickson, J.A.D., 2009. Fissure fills along faults: Variscan examples
761 from Gower, South Wales. *Geological Magazine* 146, 890–902.
- 762 Wyllie, M.R.J., Gregory, A.R., 1953. Formation factors of unconsolidated porous media: influence
763 of particle shape and effect of cementation. *Journal of Petroleum Technology* 5, 103–110.
- 764 Yilmaz, H., Oyman, T., Sonmez, F.N., Arehart, G.B., Billor, Z., 2010. Intermediate sulfidation
765 epithermal gold-base metal deposits in Tertiary subaerial volcanic rocks, Sahinli/Tespil Dere
766 (Lapseki/Western Turkey). *Ore Geology Reviews* 37, 236–258.

767 **Figure Captions**

768

769 **Fig. 1:** Illustrations of the six main hypotheses for the formation of cockade breccias: (a) cut-effect,
770 (b) crystallisation pressure, (c) suspension in fluid, (d) partial metasomatic replacement of clast
771 minerals, (e) infall of clasts during cementation and (f) repeated rotation and accretion. For detailed
772 explanations see main text.

773

774 **Fig. 2:** Maps showing the exact location of the cockade breccia occurrence on the Gower peninsula:
775 (a) Regional geological overview, with the Oxwich faults marked in; (b) map of the East Oxwich
776 fault as it outcrops on the foreshore. The sequence of the major fill generations is: (1) white calcite,
777 (2) breccia with red matrix, (3) breccia with orange matrix, (4) cockade breccia. Note that the term
778 'matrix' in this case is used to refer to all the material between individual clasts, since the distinction
779 between cement and fine-grained material is difficult in the field. Coordinates provided on (a) refer
780 to the UK ordnance survey grid. Ovals with radiating lines towards the eastern side of the vein
781 represent wall rock fragments overgrown by the first cement generation.

782

783 **Fig. 3:** Field photographs showing the cockade breccia unit: (a) sampling location, with sample
784 material still in place (the arrow marks the cockade shown in detail in Fig. 4), and (b) view to the
785 right of (a), showing the continuity of the unit. Hammer for scale. Red bands correspond to
786 haematite inclusion-rich zones.

787

788 **Fig. 4:** Line drawings of horizontal, serial sections through one cockade, taken at vertical distances
789 of c. 1 cm, with (a) being on top, and (c) at the bottom. All black lines and areas mark zones rich in
790 haematite inclusions. Sections are shown in the same orientation as the cockade was found, seen
791 from above (cf. Fig. 3a). The subdivision into cement generations I to IV followed the occurrence
792 of pronounced zones of inclusion-rich material. Shading does not reflect real variations in colour.
793 Arrows indicate small breaks in the cement layers. The photographs corresponding to these
794 drawings are shown in Fig. 5.

795

796 **Fig. 5:** Photographs corresponding to the line drawings in Fig. 4; (d) shows a schematic sketch of
797 the exact locations of the sections within the original cockade, seen from the side.

798

799 **Fig. 6:** Sedimentary nature of fine-grained haematitic material: (a) preferential coating of upward
800 directed crystal faces of cement on fault walls, (b) varying thickness across crystal tips which were
801 probably coated from above, due to sediment slumping (detail of Fig. 5b), (c) larger fragments of

802 various vein fills embedded in haematitic sediment, (d) normal grading of fragments in haematitic
803 sediment. All samples shown were taken from the East Oxwich fault, except for the one shown in
804 (a) which was taken at Limeslade Bay. Similar textures occur ubiquitously throughout the Gower
805 veins.

806

807 **Fig. 7:** Illustration of the two textural end-members resulting from multiple refracturing and
808 recementation events of a breccia body depending on the relative speed of cementation: (a)
809 formation of a cockade breccia at low relative cementation speed where fracturing of clasts is
810 mostly along cement sutures between clasts, and (b) formation of a multiphase crackle breccia,
811 where relative cementation speed is fast, resulting in the complete cementation of the clasts between
812 fracturing events. The apparent proportion of cement in the lower two thirds of the two breccia
813 bodies at stage III are 58.3% and 63.2 % for the cockade and crackle breccias, respectively.

814

815 **Fig. 8:** Schematic illustrations of eight criteria for the correct identification of cockade breccias
816 *sensu stricto*, (a) identifiable on outcrop scale, (b) identifiable on hand-specimen scale. Verification
817 of some criteria might necessitate microscopic examination. For details see main text.

Table 1 – Occurrence of cockade breccias

Type	No. of well documented occurrences ¹	Total no. of reported occurrences	Main references (well documented occurrences)
Epithermal Au-(Ag,Cu) veins	5	52	Gibson et al., 1990; Jobson et al., 1994; Genna et al., 1996; Leroy et al., 2000; Grancea et al., 2002; Squires, 2005
(Epithermal) Pb-Zn-(Cu,Ag,Sn) veins	11	25	Weissenbach, 1836; Spurr, 1926; Buerger and Maury, 1927; Ingham, 1940; Watson, 1943; Kutina and Sedlackova, 1961; Rieder, 1969; Sperling, 1973; Laznicka, 1988; Munoz et al., 1994, 1999; Bélistont et al., 2014
Fluorite-(Baryte) veins	1	10	Van Alstine, 1944
Low-T Calcite veins	1	2	Wright et al., 2009
Mesothermal veins (various)	-	2	-
Other	-	15	-

¹Containing at least either pictures of proper cockade breccias or an accurate and detailed description.

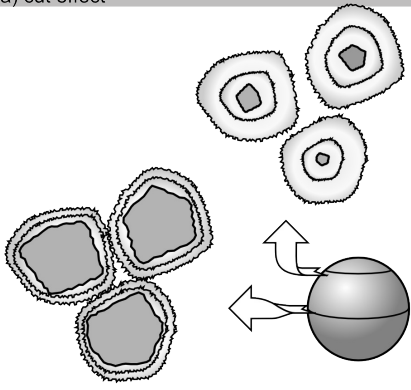
Note: A complete list of all occurrences and the references used for the compilation of this table may be found in Appendix A, in the online supplementary material.

Table 2 – Cement proportion of (true) cockade breccias

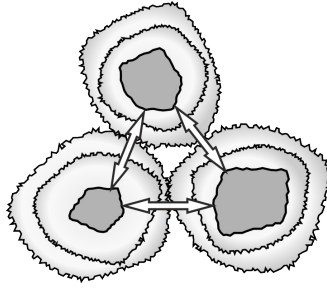
Locality	Type	Clasts touching in section?	Apparent porosity ¹	No. of clasts in sections (No. of figures)	Reference(s)
Chocaya, Bolivia	Sn-Ag veins	No	0.71	12 (1)	Buerger and Maury, 1927
Grund mine, Germany	Pb-Zn-Ag veins	No	0.65 – 0.78 (0.71)	29 (2)	Sperling 1973
Lebong Tandai mine, Indonesia	Epithermal Au veins	No	0.72	16 (1)	Jobson et al., 1994
Pribram, Czech Republic	Pb-Zn-Ag veins	No	0.75 – 0.85 (0.80)	44 (2)	Kutina and Sedlackova, 1961
Alacrán Mine, Mexico	Ag-Pb-Zn vein	No	0.72 – 0.85 (0.80)	18 (3)	Spurr, 1926
Akshiiryak deposit, Kirghizia	Pb-Zn veins	No	0.81	16 (1)	Laznicka, 1988
Cirotan, Indonesia	Epithermal Au veins	No	0.57 – 0.89 (0.79)	88 (6)	Genna et al., 1996; Leroy et al., 2000

¹Ranges are given, where several figures were analysed. The number in parantheses below the range gives the average apparent porosity of all figures.

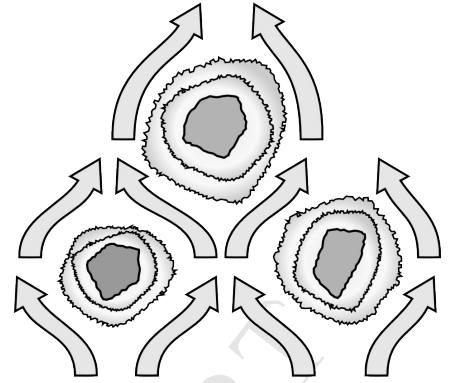
a) cut effect



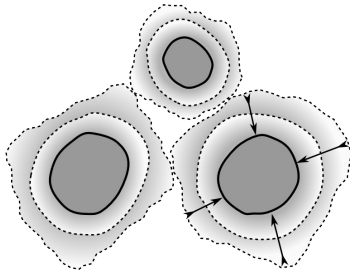
b) crystallisation pressure



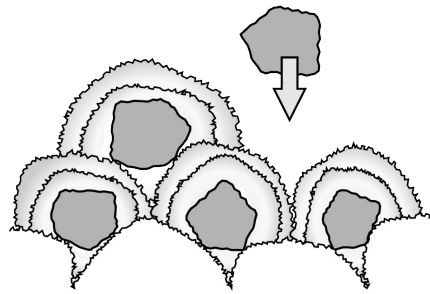
c) suspension in fluid



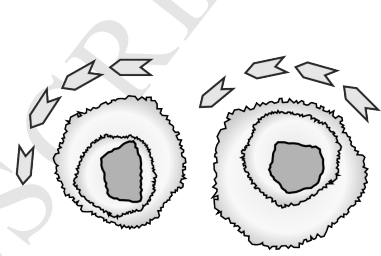
d) partial metasomatic replacement



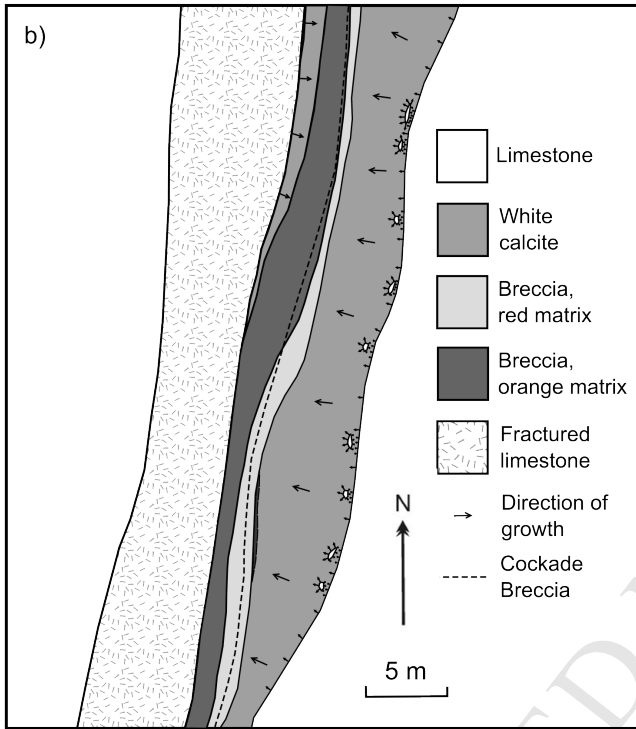
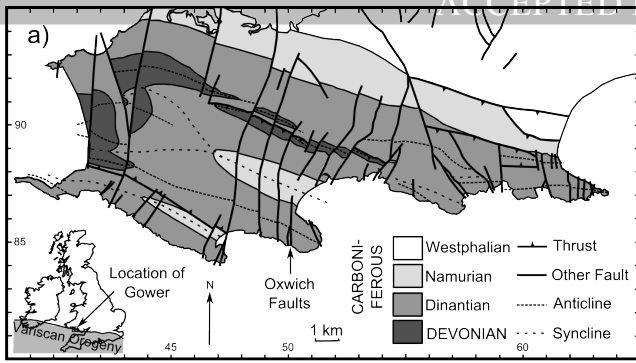
e) infall of clasts

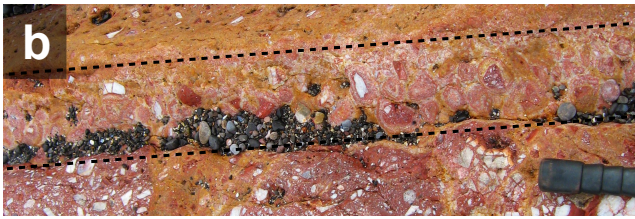
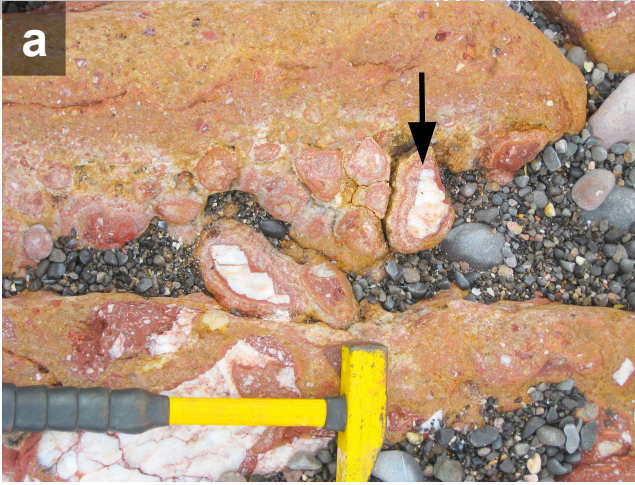


f) repeated accretion and rotation

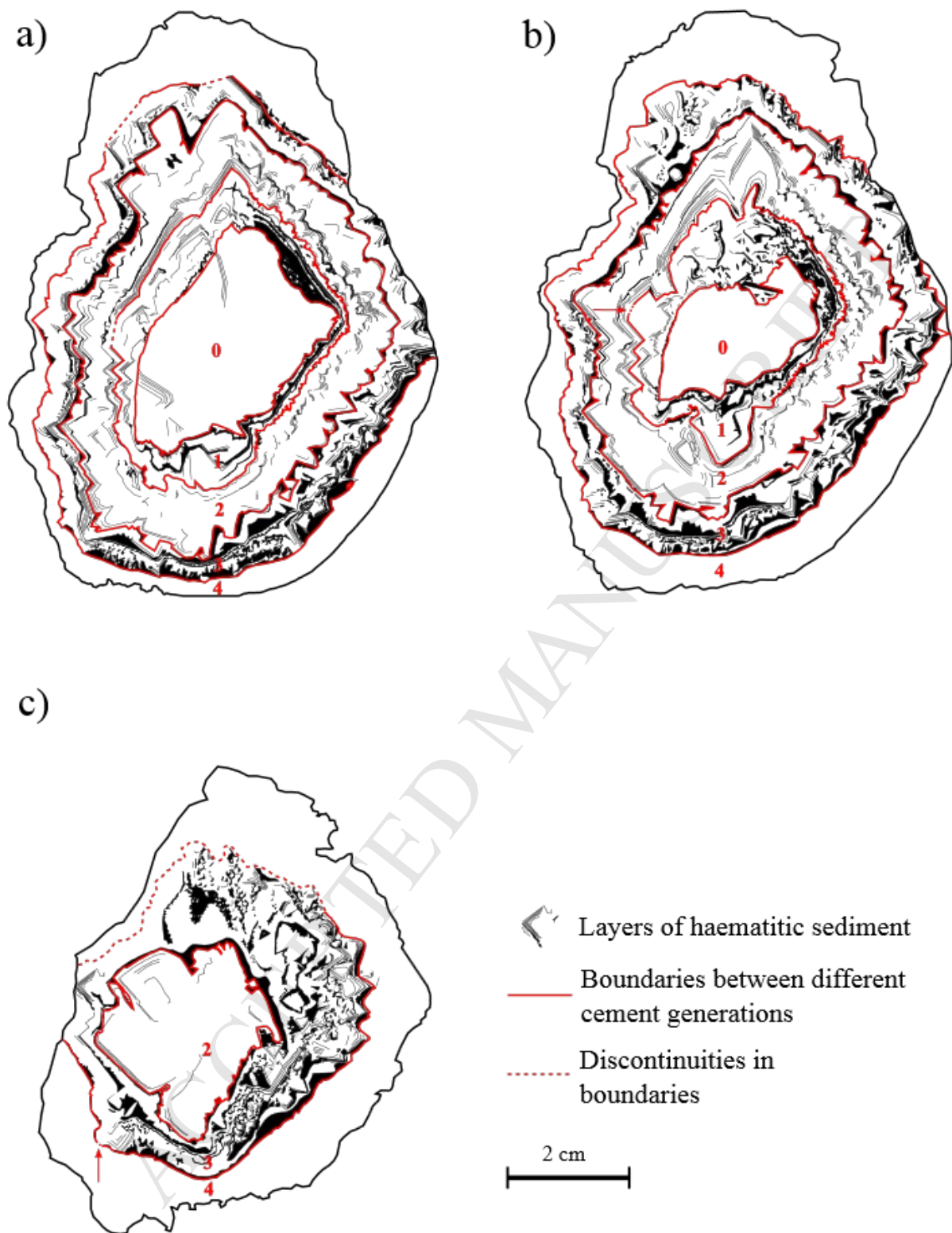


ACCEPTED MANUSCRIPT





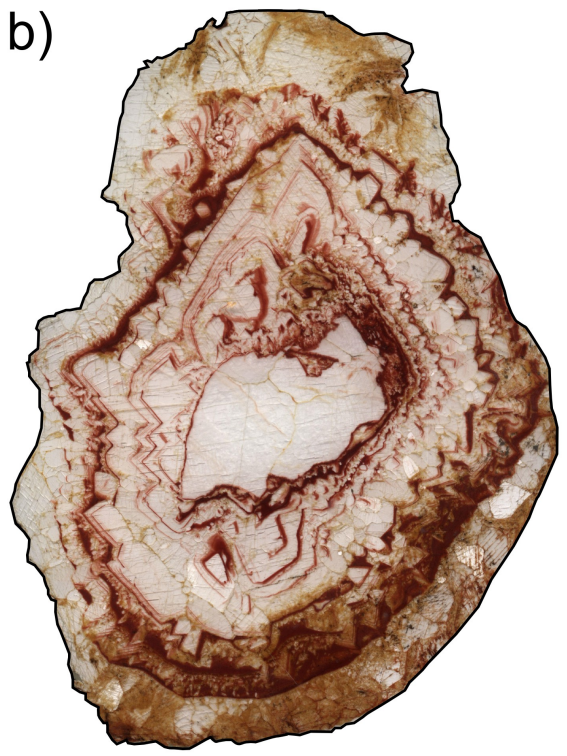
ACCEPTED MANUSCRIPT



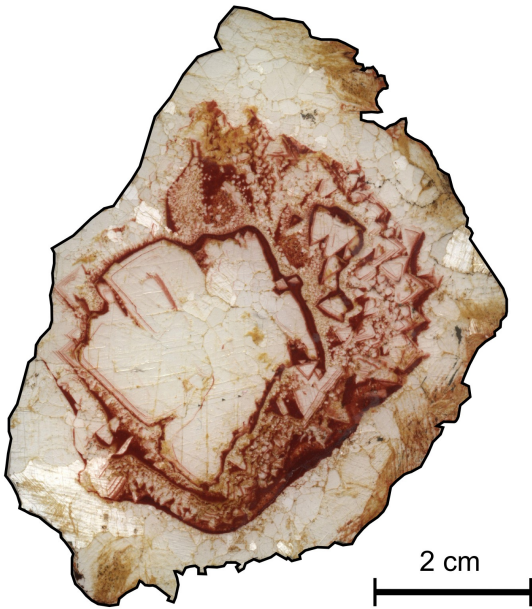
a)



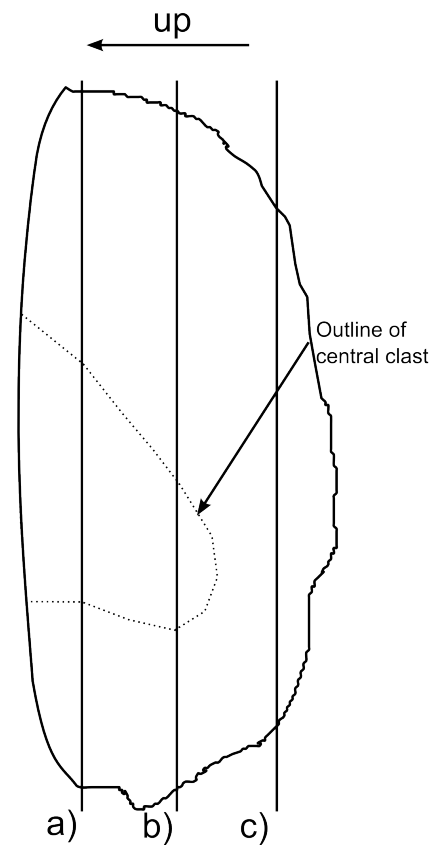
b)

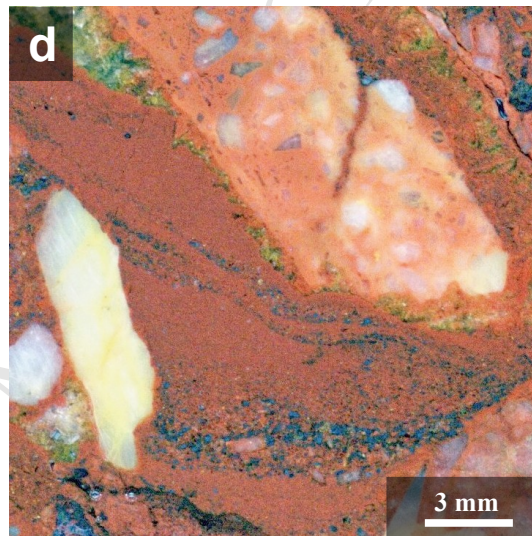
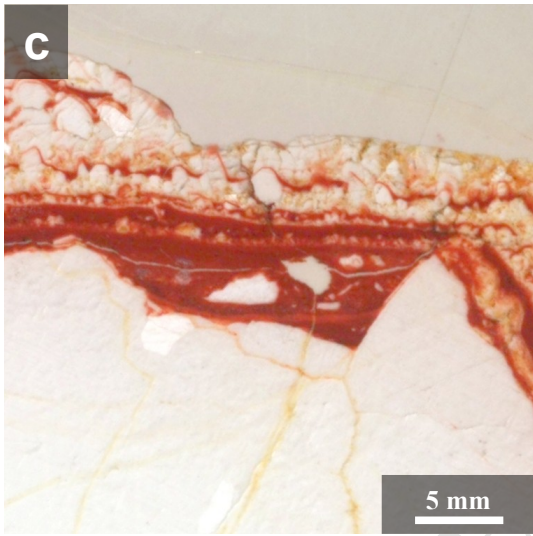
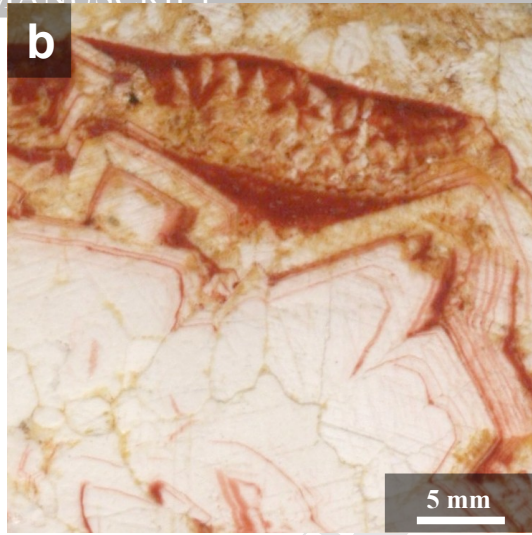
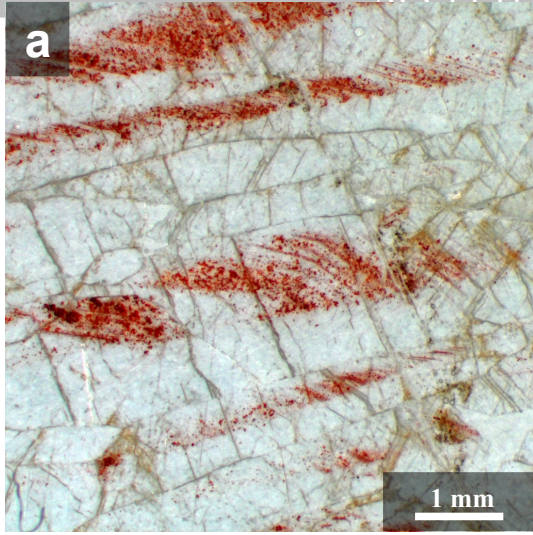


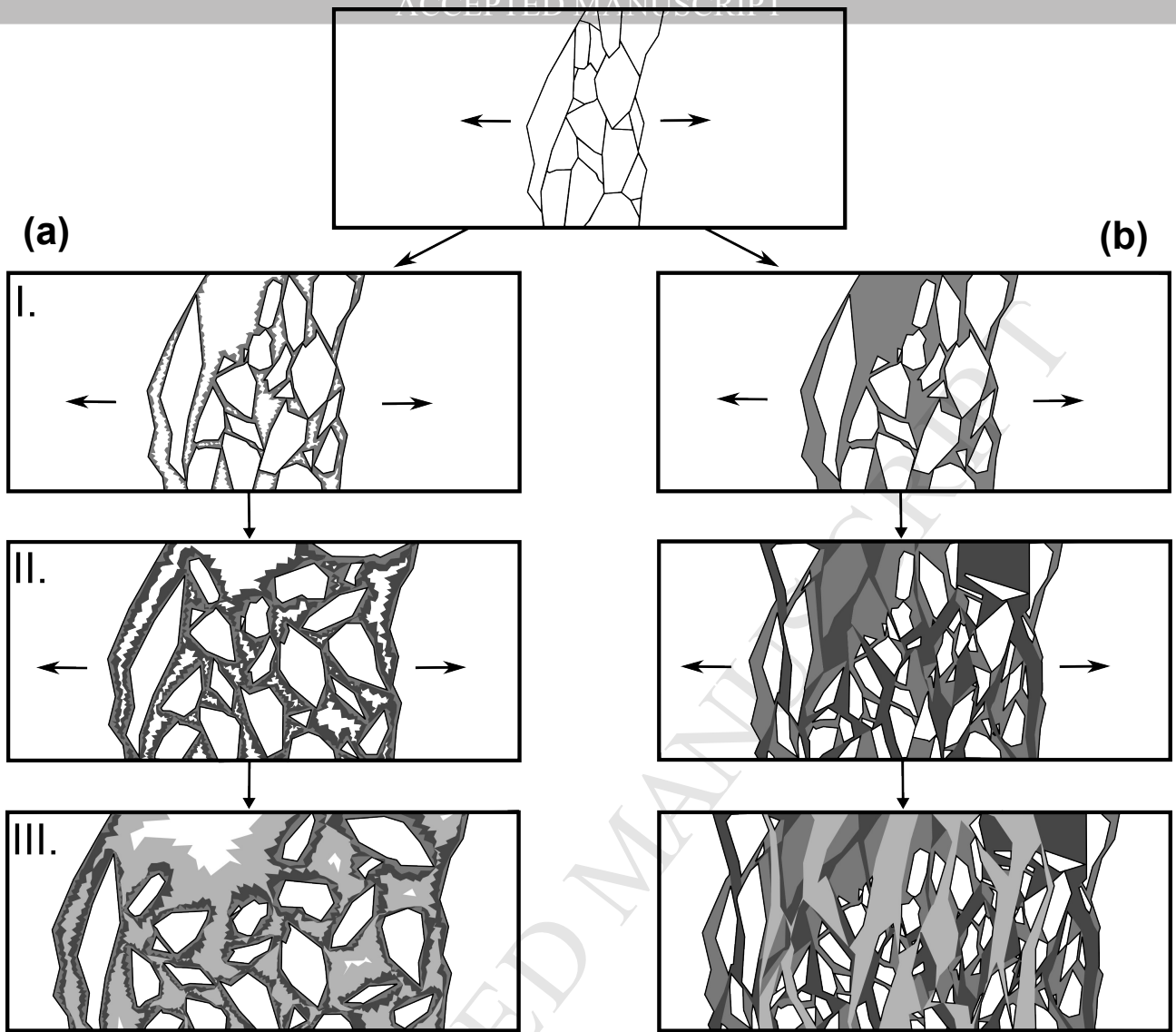
c)

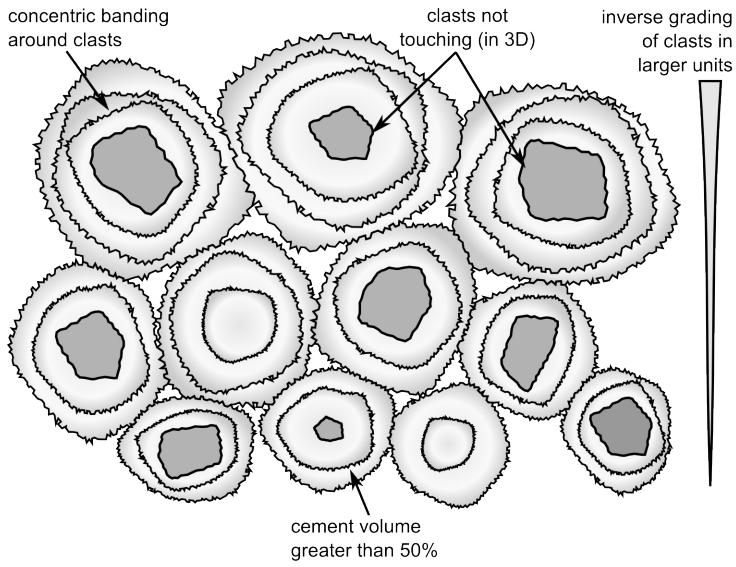
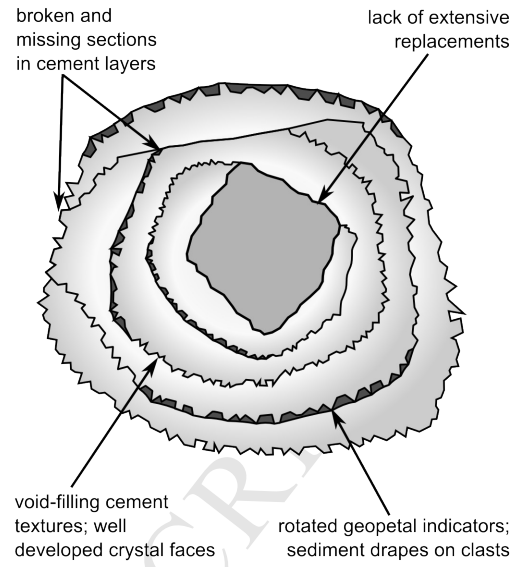


d)







a) Outcrop scale**b) Hand-specimen scale**

ACCEPTED MANUSCRIPT

Appendix A – Occurrences of cockade breccias**Table A1 – Well documented occurrences**

Type	Locality	Reference(s)
Epithermal Au- (Ag,Cu) veins	Calera, Oropampa district, Peru	Gibson et al., 1990
	Baia Mare, Romania	Grancea et al., 2002
	Exploits subzone and Gander zone, Newfoundland	Squires, 2005
	Cirotan mine, Indonesia	Genna et al., 1996; Leroy et al., 2000
	Lebong Tandai mine, Indonesia	Jobson et al., 1994
Epithermal Pb-Zn- (Cu,Ag,Au,Sn) veins	Saint-Salvy/Noailhac deposit, France	Munoz et al., 1994; Bélistont et al., 2013
	Peyrebrunne, France	Munoz et al., 1997
	Chocaya, Bolivia	Buerger and Maury, 1927
	Shawangunk Mts., New York State, USA	Ingham, 1940; Sims and Hotz, 1951; Wilbur et al., 1990; Friedman et al., 1994
	Pribram, Czech Republic	Kutina and Sedlackova, 1961
	Bad Grund, Harz Mts., Germany	Lang, 1973
	Akshiiryak, Khirgizia	Laznicka, 1988
	Bianska Stavnica, Slovakia	Rieder, 1969
	Alacran mines, Mexico	Spurr, 1926
	Port au Port Peninsula, Newfoundland, Canada	Watson, 1943
	Erzgebirge Mts., Germany	Weissenbach, 1836
Fluorite-Baryte veins	St. Lawrence, Newfoundland, Canada	Van Alstine, 1944
Low-T calcite veins	Gower Peninsula, Wales	Wright et al., 2009

Table A2 – Reported occurrences

Type	Locality	Reference(s)
Epithermal Au- (Ag,Cu) veins	Efemcukuru, Izmir, Turkey	Baba and Güngör, 2002; Oyman et al., 2003
	Golden Cross, New Zealand	Bebgie et al., 2007
	Pajingo, Queensland, Australia	Bobis et al., 1995
	Waihi, New Zealand	Braithwaite and Fauré, 2002
	Shila Cordillera, Peru	Cassard et al., 2000; Chauvet et al., 2006
	South Korea	Choi et al., 2005a,b
	Hauraki goldfield, New Zealand	Christie and Robinson, 1992
	Acupan, Baguio District, Philippines	Cooke and Bloom, 1990
	Cracow vein system, Queensland, Australia	Dong and Morrison, 1995; Dong and Zhou, 1996
	Eastern Dunnage zone, Newfoundland, Canada	Evans, 1993
	Qaleh-Zari deposit, Iran	Hassan-Nezhad and Moore, 2006
	Yatani deposit, Japan	Hattori, 1975
	Tonopah mine, Nevada, USA	Henley and Berger, 2000

Type	Locality	Reference(s)
	Comstock district, Nevada, USA	Hudson, 2003
	Ikuno mine, Japan	Jensen, 1957
	Lalab, Sibutad, Zamboanga del Norte, Philippines	Jimenez et al., 2002a,b, 2007
	Sunshin, South Korea	Kim et al., 2012
	Haenam-Jindo area, South Korea	Kim and Choi, 2009
	Ducat and Lunny orefields, Russia	Konstantinov et al., 1993
	Chah Zar deposit, Iran	Kouhestani et al., 2012, 2013
	Ozernovskoe and Praslovskoe deposits, Kuril, Kamchatka, Russia	Kovalenker and Plotinskaya, 2005
	Jinxi-Yelmand, Tianshan, Xinjiang, China	Long et al., 2005
	Guanajuato, Mexico	Mango et al., 2013
	Steep Nap prospect, Newfoundland, Canada	Mills et al., 1999
	Kiena Mine, Val D'Or, Quebec, Canada	Morasse et al., 1995
	Don Sixto deposit, Mendoza, Argentina	Mugas Lobos and Marques Zavalía, 2013
	Ohio and Mt. Baldy districts, Piute Cty., Utah, USA	Nuelle et al., 1985
	Holyrood Horst, Newfoundland, Canada	O'Brien, 2002
	Bahia Laura, Deseado Massif, Argentina	Paez et al., 2010
	Taebaeksan district, Korea	Pak et al., 2004
	El Dorado district, El Salvador	Richer et al., 2009
	Victoria deposit, Mankayan district, Luzon, Philippines	Sajona et al., 2002
	Tuvatu deposit, Fiji	Scherbarth and Spry, 2006
	Tongyoung deposits, Korea	Shelton et al., 1990
	Seigoshi district, Izu Peninsula, Japan	Shikazono, 1985
	Koryu mine, Hokkaido, Japan	Shimizu et al., 1998
	Mt. Muro Prospect, Borneo, Indonesia	Simmons and Browne, 1990
	Sierras Pampeanas, Argentina	Skirrow et al., 2000
	Esquel deposit, Argentina	Soechting et al., 2008
	Major's Creek, New South Wales, Australia	Wake and Taylor, 1988
	Hurd Peninsula, South Shetlands	Willan, 1992, 1994; Willan and Spiro, 1996
	Wadi Abu Khuhsayba, Jordan	Al-Hwaiti et al., 2010
	Gunung Pongkor deposit, West Java, Indonesia	Basuki et al., 1994
	Chahnali prospect, Baman volcano, Iran	Daliran et al., 2005
	Caylloma district, Peru	Echavarría et al., 2006
	Tombulilato district, North Sulawesi, Indonesia	Perello, 1994

Type	Locality	Reference(s)
	Promezhutochnoe deposit, Central Chukchi, Russia	Volkov and Prokofev, 2011
Epithermal Pb-Zn-(Cu,Ag,Au,Sn) veins	Milos Island, Greece	Alfieris et al., 2013
	Santo Nino Vein, Fresnillo Distr., Zacatecas, Mexico	Simmons et al., 1988; Gemmell et al., 1989
	Yatanideposit, Japan	Hattori, 1975
	Pingüino vein system, Deseado Massif, Patagonia, Argentina	Jovic et al., 2011a,b,c
	Nigadoo vein deposit, New Brunswick, Canada	Kalliokoski, 1961
	Dunbrack deposit, Musquodoboit batholith, southern Nova Scotia	Kontak et al., 1999
	Hiendelencina district, Guadalajara, Spain	Martinez Frias, 1992
	Alcudia valley, Eastern Sierra Morena, Spain	Palero-Fernandez et al., 2003; Palero Fernandez and Martin Izard, 2005
	San Vicente, Peru	Schütfort, 2001
	Sambo deposit, Korea	So et al., 1984
	Plaka Ore-System, Lavrion, Greece	Voudouris et al., 2008
	Castrovirreyana District, Central Peru	Wise, 2005
	Minas Capillitas	Marquez Zavalía, 2002; Putz et al., 2006; Paar et al., 2008; Putz et al., 2009
	Kolyma-Verkhoyansk fold belt, Russia	Anikina et al., 2003
	Assif El Mal, High Atlas, Morocco	Bouabdellah et al., 2009
Fluorite-Baryte veins	Cerro Aspero, Cordoba prov. , Argentina	Coniglio et al., 2000
	Nabburg-Wölsendorf district, SE Germany	Dill and Weber, 2010; Dill et al., 2011
	Regensburg, SE Germany	Dill et al., 2012
	Speewah, Kimberley, Australia	Gwalani et al., 2010
	Southeastern Alps, Europe	Hein et al., 1990
	Southwestern Massif Central, Albigeois, France	Munoz et al., 1999
	Valle de Tena, Pyrenees, Spain	Subias et al., 1998
	La Azul deposit, Taxco district, Mexico	Tritlla and Levresse, 2006
	Santa Catarina State, Brazil	Jelinek et al., 1999
Low-T calcite veins	Southern Arizona	Davis et al., 1979
Mesothermal veins (various)	Salsigne deposit, France	Demange et al., 2006
	Bilimoia, Kainantu region, Papua New Guinea	Espi et al., 2007
Orogenic/Epizonal gold deposits	Red-Lake/Campbell mine, Canada	Penczak and Mason, 1997; Tarnocai et al., 1998; Penczak and Mason, 1999; Dubé et al., 2004; Chi et al., 2009
	Donlin Creek, Alaska, USA	Goldfarb et al., 2004

Type	Locality	Reference(s)
	Yilgarn Craton, Western Australia	Groves, 1993; Groves et al., 1998; Bateman and Hagemann, 2004
	Wiluna, Western Australia	Hagemann and Lüders, 2003
	Kalgoorlie district, Western Australia	Mueller et al., 1988, 2013
<i>MVT</i>	<i>Zawar, India</i>	<i>Mookherjee, 1964</i>
	<i>County Tipperary, Ireland</i>	<i>Wilkinson and Lee, 2003</i>
	<i>Southwestern Sardinia, Italy</i>	<i>Boni and Malafronte, 1983; Boni, 1986; Boni et al., 1988</i>
	<i>Howell, Jefferson County, USA</i>	<i>Ludlum, 1955</i>
	<i>Bleiberg</i>	<i>Schroll et al., 1983</i>
IOCG	Oak Dam East, Galwer Craton, Australia	Davidson et al., 2007
	Contact Lake Belt, Northwestern Territories, Canada	Mumin et al., 2007
Calcite cemented calamine breccia	High Atlas, Morocco	Choulet et al., 2014
U-Ni-Co-As-Ag/Bi veins	Zalesi deposit, Czech Republic	Dolnicek et al., 2009
Low-T quartz-fluorite-pyrite-chlorite-siderite veins	South Crofty mine, Cornwall, UK	Dominy et al., 1994
Cassiterite veins	Rosevale Mine, Zennor, West Cornwall	Dominy et al., 1995
<i>Karst collapse breccias</i>	<i>Egypt</i>	<i>El-Aref et al., 1986; El-Sharkawi et al., 1990</i>
Hydrothermal Mn/Fe-Mn deposits	Baft, Kerman, Iran	Heshmatbehzadi and Shahabpour, 2010
Quartz veins in granite	Southwest Avalon zone, Newfoundland, Canada	O'Driscoll and Strong, 1979
<i>Phreatic breccias</i>	<i>Southern Alps, Italy</i>	<i>Servida et al., 2010</i>
	-	<i>Tamas and Milesi, 2003</i>
Au-Sb veins	Loddiswell, Devon, UK	Stanley et al., 1990
Unmineralised epithermal veins	Ixtacamaxtitlan, Puebla State, Mexico	Tritlla et al., 2004

Note: Occurrences in italics were not included with the counts in Table 1, since it was thought that they did likely not represent proper cockade breccias.

References

- Al-Hwaiti, M., Zoheir, B., Lehmann, B., Rabba, I., 2010. Epithermal gold mineralisation at Wadi Abu Khushayba, southwestern Jordan. *Ore Geology Reviews* 38, 101–112.
- Alfieris, D., Voudouris, P., Spry, P.G., 2013. Shallow submarine epithermal Pb-Zn-Cu-Au-Ag-Te mineralization on western Milos Island, Aegean Volcanic Arc, Greece: Mineralogical geological and geochemical constraints. *Ore Geology Reviews* 53, 159–180.
- Anikina, E.Y., Bortnikov, N.S., Gamyarin, G.N., 2003. Rhythmical and banded veins at silver-lead-zinc deposits of the Kolyma-Verkhoyansk fold belt, Russia: Implications for fluid boiling. In: *Proceedings of the 7th Biennial meeting of the Society of Geology Applied to Mineral Deposits, Mineral exploration and sustainable development, Proceedings*, 433–436.

- Baba, A., Güngör, T., 2002. Influence of gold-mine on groundwater quality (Efemcukuru, Izmir, Turkey). *Environmental Geology* 41, 621–627.
- Basuki, A., Sumanagara, D.A., Sinambela, D., 1994. The Gunung Pongkor gold-silver deposit, West Java, Indonesia. *Journal of Geochemical Exploration* 50, 371–391.
- Bateman, R., Hagemann, S., 2004. Gold mineralisation throughout 45 Ma of Archaean orogenesis: protracted flux of gold in the Golden Mile, Yilgarn craton, Western Australia. *Mineralium Deposita* 39, 536–559.
- Bebgie, M.J., Spörli, K.B., Mauk, J.L., 2007. Structural evolution of the Golden Cross epithermal Au-Ag deposit, New Zealand. *Economic Geology* 102, 873–892.
- Bélissont, R., Boiron, M.-C., Luais, B., Cathelineau, M., 2014. LA-ICP-MS analyses of minor and trace elements and bulk Ge isotopes in zoned Ge-rich sphalerites from the Noailhac – Saint-Salvy deposit (France): insights into incorporation mechanisms and ore deposition processes. *Geochimica et Cosmochimica Acta* 126, 518–540.
- Bobis, R.E., Jaireth, S., Morrison, G.W., 1995. The anatomy of a Carboniferous epithermal ore shoot at Pajingo, Queensland: setting, zoning, alteration, and fluid conditions. *Economic Geology* 90, 1776–1798.
- Boni, M., 1986. The Permo-Triassic vein and paleokarst ores in southwest Sardinia: Contribution of fluid inclusion studies to their genesis and paleoenvironment: *Mineralium Deposita* 21, 53–62.
- Boni, M., Iannace, A., Pierre, C., 1988. Stable-isotope compositions of Lower Cambrian Pb-Zn-Ba deposits and their host carbonates, southwestern Sardinia, Italy. *Chemical Geology* 72, 267–282.
- Boni, M., Malafrente, A., 1983. Structural setting and genesis of ore bodies in carbonate rocks in the M.te Atzei – M.te Ega mining area (Sulcis, SW Sardinia). *Mineralium Deposita*, 18, 57–69.
- Bouabdellah, M., Beaudoin, G., Leach, D.L., Grandia, F., Cardellach, E., 2009. Genesis of the Assif El Mal Zn-Pb (Cu, Ag) vein deposit. An extension-related Mesozoic vein system in the High Atlas of Morocco. Structural, mineralogical, and geochemical evidence. *Mineralium Deposita* 44, 689–704.
- Braithwaite, R.L., Faure, K., 2002. The Waihi epithermal gold-silver-base metal sulfide-quartz vein system, New Zealand: temperature and salinity controls on electrum and sulfide deposition. *Economic Geology* 97, 269–290.
- Buerger, M.J., Maury, J.L., 1927. The ores of Chocaya, Bolivia. *Economic Geology* 22, 1–13.
- Cassard, D., Chauvet, A., Bailly, L., Llosa, F., Rosas, J., Marcoux, E., Lerouge, C., 2000. Structural control and K/Ar dating of the Au-Ag epithermal veins in the Shila Cordillera, southern Peru. *Earth and Planetary Sciences* 330, 23–30.
- Chauvet, A., Bailly, L., André, A.-S., Monié, P., Cassard, D., Llosa Tajada, F., Rosas Vargas, J., Tuduri, J., 2006. Internal vein texture and vein evolution of the epithermal Shila-Paula district, southern Peru. *Mineralium Deposita* 41, 387–410.
- Chi, G., Liu, Y., Dubé, B., 2009. Relationship between CO₂-dominated fluids, hydrothermal alterations and gold mineralization in the Red Lake greenstone belt, Canada. *Applied Geochemistry* 24, 504–516.
- Choi, S.-G., Kwon, S.-T., Ree, J.-H., So, C.-S., Pak, S.J., 2005. Origin of Mesozoic gold mineralization in South Korea. *The Island Arc* 14, 102–114.
- Choi, S.-G., Ryu, I.-C., Pak, S.J., Wee, S.-M., Kim, C.S., Park, M.-E., 2005. Cretaceous epithermal gold-silver mineralization and geodynamic environment, Korea. *Ore Geology Reviews* 26, 115–135.
- Choulet, F., Charles, N., Barbanson, L., Branquet, Y., Sizaret, S., Ennaciri, A., Badra, L., Chen, Y., 2014. Non-sulfide zinc deposits of the Moroccan High-Atlas: Multi-scale characterization and origin. *Ore Geology Reviews* 56, 115–140.
- Christie, A.B., Robinson, B.W., 1992. Regional sulphur isotope studies of epithermal Au-Ag-Pb-Zn-Cu deposits in the Hauraki Goldfield, South Auckland. *New Zealand Journal of Geology and*

Geophysics 35, 145–150.

- Coniglio, J., Xavier, R.P., Pinotti, L., D'Eramo, F., 2000. Ore-forming fluids of vein-type fluorite deposits of the Cerro Aspero batholith, southern Cordoba province, Argentina. *International Geology Review* 42, 368–383.
- Cooke, D.R., Bloom, M.S., 1990. Epithermal and subjacent porphyry mineralization, Acupan, Baguio District, Philippines: a fluid-inclusion and paragenetic study. *Journal of Geochemical Exploration* 35, 297–340.
- Daliran, F., Paar, W.H., Neubauer, F., Rashidi, B., 2005. New discovery of epithermal gold at Chahnali prospect, Baman volcano, SE-Iran. 8th Biennial SGA Meeting, Mineral Deposit Research: Meeting the Global Challenge, Beijing, China, Proceedings, 917–919.
- Davidson, G.J., Paterson, H., Meffre, S., Berry, R.F., 2007. Characteristics and origin of the Oak Dam East breccia-hosted, iron oxide Cu-U-(Au) deposit: Olympic Dam region, Gawler Craton, south Australia. *Economic Geology* 102, 1471–1498.
- Davis, G.H., Phillips, M.P., Reynolds, S.J., Varga, R.J., 1979. Origin and provenance of some exotic blocks in Lower Mesozoic red-bed basin deposits, southern Arizona. *Geological Society of America Bulletin* 90, 376–384.
- Demange, M., Pascal, M.-L., Raimbault, L., Armand, J., Forette, M.C., Serment, R., Touil, A., 2006. The Salsigne Au-As-Bi-Ag-Cu deposit, France. *Economic Geology* 101, 199–234.
- Dill, H.G., Hansen, B.T., Weber, B., 2011. REE contents, REE minerals and Sm/Nd isotopes of granite- and unconformity-related fluorite mineralization at the western edge of the Bohemian Massif: With special reference to the Nabburg-Wölsendorf District, SE Germany. *Ore Geology Review* 40, 132–148.
- Dill, H.G., Weber, B., 2010. Variation of color, structure and morphology of fluorite and the origin of the hydrothermal F-Ba deposits at Nabburg-Wölsendorf, SE Germany. *Neues Jahrbuch für Mineralogie – Abhandlungen* 187, 113–132.
- Dill, H.G., Weber, B., Eigler, G., Kaufhold, S., 2012. The fluorite deposits NE of Regensburg, SE Germany – A mineralogical and chemical comparison of unconformity-related fluorite vein-type deposits. *Chemie der Erde* 72, 261–278.
- Dolnicek, Z., Fojt, B., Prochaska, W., Kucera, J., Sulovsky, P., 2009. Origin of Zálesí U-Ni-Co-As-Ag/Bi deposit, Bohemian Massif, Czech Republic: fluid inclusion and stable isotope constraints. *Mineralium Deposita* 44, 81–97.
- Dominy, S.C., Camm, G.S., Bussell, M.A., Bennett, T.S., 1995. The structure and paragenetic evolution of cassiterite mineralized veins at Rosevale Mine, Zennor, West Cornwall. *Proceedings of the Ussher Society* 8, 374–378.
- Dominy, S.C., Scrivener, R.C., Le Boutillier, N., Bussell, M.A., Halls, C., 1994. Crosscourses in South Crofty Mine, Cornwall: further studies of paragenesis and structure. *Proceedings of the Ussher Society* 8, 237–241.
- Dong, G., Morrison, G.W., 1995. Adularia in epithermal veins, Queensland: morphology, structural state and origin. *Mineralium Deposita* 30, 11–19.
- Dong, G.Y., Zhou, T., 1996. Zoning in the Carboniferous-Lower Permian Cracow epithermal vein system, central Queensland, Australia. *Mineralium Deposita* 31, 210–244.
- Dubé, B., Williamson, K., McNicoll, V., Malo, M., Skulski, T., Twomey, T., Sanborn-Barrie, M., 2004. Timing of gold mineralization at Red Lake, Northwestern Ontario, Canada: New Constraints from U-Pb geochronology at the Goldcorp high-grade zone, Red Lake Mine, and the Madsen Mine. *Economic Geology* 99, 1611–1641.
- Echavarria, L., Nelson, E., Humphrey, J., Chavez, J., Escobedo, L., Iriando, A., 2006. Geologic evolution of the Caylloma epithermal vein district, Southern Peru. *Economic Geology* 101, 843–863.
- El Aref, M.M., Awadallah, F., Ahmed, S., 1986. Karst landform development and related sediments in the Miocene rocks of the Red Sea coastal zone, Egypt. *Geologische Rundschau* 75, 781–790.
- El Sharkawi, M.A., El Aref, M.M., Abdel Motelib, A., 1990. Manganese deposits in a

- Carboniferous paleokarst profile, Um Bogma region, west-central Sinai, Egypt. *Mineralium Deposita* 25, 34–43.
- Espi, J.O., Hayashi, K.-I., Komuro, K., Murakami, H., Kajiwar, Y., 2007. Geology, wall-rock alteration and vein paragenesis of the Bilimoia gold deposit, Kainantu metallogenic region, Papua New Guinea. *Resource Geology* 57, 249–268.
- Evans, D.T.W., 1993. Gold mineralization in the eastern Dunnage Zone, central Newfoundland. Newfoundland Department of Mines and Energy, Geological Survey Branch Report 93-1, 339–349.
- Friedman, J.D., Conrad, J.E., McKee, E.H., Mutschler, F.E., Zartmann, R.E., 1994. Possible Mesozoic age of Ellenville Zn-Pb-Cu(Ag) deposit, Shawangunk Mountains, New York. *Mineralium Deposita* 29, 474–478.
- Gemmell, J.B., Zantop, H., Birnie, R.W., 1989. Silver sulfosalts of the Santo Nino Vein, Fresnillo District, Zacatecas, Mexico. *Canadian Mineralogist* 27, 401–418.
- Genna, A., Jébrak, M., Marcoux, E., Milési, J.P., 1996. Genesis of cockade breccias in the tectonic evolution of the Cirotan epithermal gold system, West Java. *Canadian Journal of Earth Sciences* 33, 93–102.
- Gibson, P.C., Noble, D.C., Larson, L.T., 1990. Multistage evolution of the Calera epithermal Ag-Au vein system, Orcopampa District, southern Peru: First results. *Economic Geology* 85, 1504–1519.
- Goldfarb, R.J., Ayuso, R., Miller, M.L., Ebert, S.W., Marsh, E.E., Petsel, S.A., Miller, L.D., Bradley, D., Johnson, C., McClelland W., 2004. The Late Cretaceous Donlin Creek gold deposit, southwestern Alaska: Controls on epizonal ore formation. *Economic Geology* 99, 643–671.
- Grancea, L., Bailly, L., Leroy, J., Banks, D., Marcoux, E., Milési, J.P., Cuney, M., André A.S., Istvan, D., Fabre, C., 2002. Fluid evolution in the Baia Mare epithermal gold/polymetallic district, Inner Carpathians, Romania. *Mineralium Deposita* 37, 630–647.
- Groves, D.I., 1993. The crustal continuum model for late-Archaeon lode-gold deposits of the Yilgarn Block, Western Australia. *Mineralium Deposita* 28, 366–374.
- Groves, D.I., Goldfarb, R.J., Gebre-Mariam, M., Hagemann, S.G., Robert, F., 1998. Orogenic gold deposits: A proposed classification in the context of their crustal distribution and relationship to other gold deposit types. *Ore Geology Reviews* 13, 7–27.
- Gwalani, L.G., Rogers, K.A., Demény A., Groves, D.I., Ramsay, R., Beard, A., Downes, P.J., Eves, A., 2010. The Yungul carbonatite dykes associated with the epithermal fluorite deposit at Speewah, Kimberley, Australia: carbon and oxygen isotope constraints on their origin. *Mineralogy and Petrology* 98, 123–141.
- Hagemann, S.G., Lüders, V., 2003. P-T-X conditions of hydrothermal fluids and precipitation mechanism stibnite-gold mineralization at the Wiluna lode-gold deposits, Western Australia: conventional and infrared microthermometric constraints. *Mineralium Deposita* 38, 936–952.
- Hassan-Nezhad, A.A., Moore, F., 2006. A stable isotope and fluid inclusion study of the Qaleh-Zari Cu-Au-Ag deposit, Khorasan province, Iran. *Journal of Asian Earth Sciences* 27, 805–818.
- Hattori, K., 1975. Geochemistry of ore deposition at the Yatani lead-zinc and gold-silver deposit, Japan. *Economic Geology* 70, 677–693.
- Hein, U.F., Lüders, V., Dulski, P., 1990. The fluorite vein mineralization of the southern Alps: combined application of fluid inclusions and rare earth element (REE) distribution. *Mineralogical Magazine* 54, 325–333.
- Henley, R.W., Berger, B.R., 2000. Self-ordering and complexity in epizonal mineral deposits. *Annual Review of Earth and Planetary Sciences* 28, 669–719.
- Heshmatbehzadi, K., Shahabpour, J., 2010. Metallogeny of manganese and ferromanganese ores in Baft ophiolitic mélange, Kerman, Iran. *Australian Journal of Basic and Applied Sciences* 4, 302–313.
- Hudson, D.M., 2003. Epithermal alteration and mineralization in the Comstock District, Nevada.

Economic Geology 98, 367–385.

- Ingham, A.I., 1940. The zinc and lead deposits of Shawangunk Mountain, New York. *Economic Geology* 35, 751–760.
- Jelinek, A.R., Bastos Neto, A.C., Lelarge, M.L.V., Soliani, E. Jr., 1999. Apatite fission track dating of fluorite ore veins from Santa Catarina state, Brazil: a complex hydrothermal evolution. *Journal of South American Earth Sciences* 12, 367–377.
- Jensen, M.L., 1957. Sulfur isotopes and mineral paragenesis. *Economic Geology* 52, 269–281.
- Jimenez, F.A., Yumul, G.P., Maglambayan, V.B., 2002. Gold and base-metal sulfide mineralogy and paragenesis of the Lalab orebody, Sibutad, Zamboanga del Norte, Philippines: Clues to the fluid composition and formation of gold-rich zones. *International Geology Review* 44, 956–971.
- Jimenez, F.A., Yumul, G.P., Maglambayan, V.B., Tamayo, R.A., 2002. Shallow to near-surface, vein-type epithermal gold mineralization at Lalab in the Sibutad gold deposit, Zamboanga del Norte, Mindanao, Philippines. *Journal of Asian Earth Sciences* 21, 119–133.
- Jimenez, F.A., Yumul, G.P., Maglambayan, V.B., 2007. Fluid inclusion microthermometry and implications for the mechanisms of ore-grade gold mineralization in epithermal system, Lalab orebody, Sibutad, Zamboanga del Norte, Philippines. *Resource Geology* 57, 170–179.
- Jobson, D.H., Boulter, C.A., Foster, R.P., 1994. Structural controls and genesis of epithermal gold-bearing breccias at the Lebong Tandai mine, Western Sumatra, Indonesia. *Journal of Geochemical Exploration* 50, 409–428.
- Jovic, S.M., Guido D.M., Ruiz, R., Páez, G.N., Schalamuk, I.B., 2011a. Indium distribution and correlations in polymetallic veins from Pingüino deposit, Deseado Massif, Patagonia, Argentina. *Geochemistry, Exploration, Environment, Analysis* 11, 107–115.
- Jovic, S.M., Guido, D.M., Melgarejo, J.C., Páez, G.N., Ruiz, R., Schalamuk, I.B., 2011b. The indium-bearing minerals of the Pingüino polymetallic vein system, Deseado massif, Patagonia, Argentina. *Canadian Mineralogist* 49, 931–946.
- Jovic, S.M., Guido, D.M., Schalamuk, I.B., Ríos, F.J., Tassinari, C.C.G., Recio, C., 2011c. Pingüino In-bearing polymetallic vein deposit, Deseado massif, Patagonia, Argentina: characteristics of mineralization and ore-forming fluids. *Mineralium Deposita* 46, 257–271.
- Kalliokoski, J., 1961. Temperatures of formation and origin of the Nigadoo and Brunswick mining and smelting No. 6 deposits, New Brunswick, Canada. *Economic Geology* 56, 1446–1455.
- Kim, K.H., Lee, S., Nagao, K., Sumino, H., Yang, K., Lee, J.I., 2012. He-Ar-H-O isotopic signatures in Au – Ag bearing ore fluids of the Sunshin epithermal gold-silver deposits, South Korea. *Chemical Geology* 320-321, 128–139.
- Kim, C.S., Choi, S.-G., 2009. Potassium-Argon ages of the epithermal gold-silver mineralization in the Haenam-Jindo area, southwestern Korea. *Resource Geology* 59, 415–421.
- Konstantinov, M.M., Rosenblum, I.S., Strujkov, S.F., 1993. Types of epithermal silver deposits, northeastern Russia. *Economic Geology* 88, 1797–1809.
- Kontak, D.J., Ansdell, K., Archibald, D., 1999. New constraints on age and origin of the Dunbrack Pb-Cu-Zn-Ag deposit, Musquodoboit batholith, southern Nova Scotia. *Atlantic Geology* 35, 29–42.
- Kouhestani, H., Ghaderi, M., Zaw, K., Meffre, S., Emami, M.H., 2012. Geological setting and timing of the Chah Zard breccia-hosted epithermal gold-silver deposit in the Tethyan belt of Iran. *Mineralium Deposita* 47, 425–440.
- Kouhestani, H., Ghaderi, M., Chang, Z., Zaw, K., 2013. Constraints on the ore fluids in the Chah Zar breccia-hosted epithermal Au-Ag deposit, Iran: fluid inclusions and stable isotope studies. *Ore Geology Reviews* (in press).
- Kovalenker, V.A., Plotinskaya, O.Y., 2005. Te and Se mineralogy of Ozernovskoe and Prasolovskoe epithermal gold deposits, Kuril–Kamchatka volcanic belt. *Geochemistry, Mineralogy and Petrology* 43, 118–123.
- Kutina, J., Sedlackova, J., 1961. The role of replacement in the origin of some cockade textures. *Economic Geology* 56, 149–176.

- Laznicka, P., 1988. Breccias and coarse fragmentites: petrology, environments, associations, ores. *Developments in Economic Geology* 25, Elsevier, Amsterdam.
- Leroy, Jacques L., Hubé, Daniel, Marcoux, E., 2000. Episodic deposition of Mn-minerals in cockade breccia structures in three low-sulfidation epithermal deposits: a mineral stratigraphy and fluid inclusion approach. *The Canadian Mineralogist* 38, 1125–1136.
- Long, X., Hayward, N., Begg, G., Minlu, F., Fangzheng, W., Pirajno, F., 2005. The Jinxi-Yelmand high-sulfidation epithermal gold deposit, western Tianshan, Xinjiang province, P.R. China. *Ore Geology Reviews* 26, 17–37.
- Ludlum, J.C., 1955. Regional setting and mineralogic features of the Howell zinc prospect, Jefferson County, W. Va. *Economic Geology* 50, 855–861.
- Mango, H., Arehart, G., Oreskes, N., Zantop, H., 2013. Origin of epithermal Ag-Au-Cu-Pb-Zn mineralization in Guanajuato, Mexico. *Mineralium Deposita* (in press, doi: 10.1007/s00126-0130478-z).
- Marquez Zavalia, M.F., 2002. Mina Capillitas, an epithermal deposit from Northwestern Argentina/Mina Capillitas, un depósito epitermal del noroeste argentino. In: IANIGLA, 30 años de investigación básica y aplicada en ciencias, Mendoza, 249–253.
- Martinez Frías, J., 1992. The Hiendelencina mining district (Guadalajara, Spain). *Mineralium Deposita* 27, 206–212.
- Mills, J., O'Brien, S.J., Dubé, B., Mason, R., O'Driscoll, C.F., 1999. The Steep Nap Prospect: A low-sulfidation, gold-bearing epithermal vein system of late Neoproterozoic age, Avalon Zone, Newfoundland and Appalachians. *New Foundland Department of Mines and Energy Geological Survey Report 99-1*, 255–274.
- Mookherjee, A., 1964. The geology of the Zawar lead-zinc mine, Rajasthan, India. *Economic Geology* 59, 656–677.
- Morasse, S., Wasteneys, H.A., Cormier, M., Helmstaedt, H., Mason, R., 1995. A pre-2686 Ma intrusion-related gold deposit at the Kiena Mine, Val D'Or, Québec, southern Abitibi subprovince. *Economic Geology* 90, 1310–1321.
- Mueller, A.G., Harris, L.B., Lungan, A., 1988. Structural control of greenstone-hosted gold-mineralization by transcurrent shearing: A new interpretation of the Kalgoorlie mining district, Western Australia. *Ore Geology Reviews* 3, 359–387.
- Mueller, A.G., Muhling, J.R., 2013. Silver-rich telluride mineralization at Mount Charlotte and Au-Ag zonation in the giant Golden Mile deposit, Kalgoorlie, Western Australia. *Mineralium Deposita* 48, 295–311.
- Mugas Lobos, A.C., Marquez-Zavalia, M.F., 2013. Fluid inclusion and stable isotope studies at Don Sixto, a precious metal low sulfidation deposit in Mendoza Province, Argentina. *Resource Geology* 63, 350–359.
- Mumin, A.H., Corriveau, L., Somarin, A.K., Ootes, L., 2007. Iron oxide copper-gold-type polymetallic mineralization in the Contact Lake Belt, Great Bear magmatic zone, Northwest Territories, Canada. *Exploration and Mining Geology* 16, 187–208.
- Munoz, M., Boyce, A.J., Courjault-Rade, P., Fallick, A.E., Tollon, F., 1994. Multi-stage fluid incursion in the Palaeozoic basement-hosted Saint-Salvy ore deposit (NW Montagne Noire, southern France). *Applied Geochemistry* 9, 609–626.
- Munoz, M., Boyce, A., Courjault-Rade, P., Fallick, A., Tollon, F., 1997. Le filon (Zn, F) de Peyrebrune (SW Massif central, France): caractérisation géochimique des fluides au cours du Mésozoïque à la bordure orientale du bassin d'Aquitaine. *Comptes Rendus de l'Académie de Sciences Paris* 324, 899–906.
- Munoz, M., Boyce, A.J., Courjault-Rade, P., Fallick, A.E., Tollon, F., 1999. Continental basinal origin of ore fluids from southwestern Massif Central fluorite veins (Albigeois, France): evidence from fluid inclusion and stable isotope analyses. *Applied Geochemistry* 14, 447–458.
- Nuelle, L.M., Proctor, P.D., Grant, S.K., 1985. Vein formation and distribution, Ohio and Mt. Baldy districts, Marysvale, Piute County, Utah, USA. *Mineralium Deposita* 20, 127–134.

- O'Brien, S.J., 2002. A note on Neoproterozoic gold, early Paleozoic copper and basement-cover relationships on the margins of the Holyrood Horst, southeastern Newfoundland. Newfoundland Department of Mines and Energy Geological Survey Report 02-1, 219–227.
- O'Driscoll, C.F., Strong, D.F., 1979. Geology and geochemistry of Late Precambrian volcanic and intrusive rocks of southwestern Avalon zone in Newfoundland. *Precambrian Research* 8, 19–48.
- Oyman, T., Minareci, F., Piskin, Ö., 2003. Efemcukuru B-rich epithermal gold deposit (Izmir, Turkey). *Ore Geology Reviews* 23, 35–53.
- Paar, W.H., Moelo, Y., Mozgova, N.N., Organova, N.I., Stanley, C.J., Roberts, A.C., Culetto, F.J., Effenberger, H.S., Topa, D., Putz, H., Sureda, R.J., de Brodtkorb, M.K., 2008. Coiraitite, (Pb, Sn²⁺)_{12.5}As₃Fe²⁺Sn₅⁴⁺S₂₈: a franckeite-type new mineral species from Jujuy Province, NW Argentina. *Mineralogical Magazine* 72, 1083–1101.
- Paez, G.N., Ruiz, R., Guido, D.M., Jovic, S.M., Schalamuk, I.B., 2010. The effects of K-metasomatism in the Bahía Laura volcanic complex, Deseado Massif, Argentina: petrologic and metallogenic consequences. *Chemical Geology* 273, 300–313.
- Pak, S.J., Choi, S.-G., Choi, S.-H., 2004. Systematic mineralogy and chemistry of gold-silver vein deposits in the Taebaeksan district, Korea: Distal relatives of a porphyry system. *Mineralogical Magazine* 68, 467–487.
- Palero-Fernandez, J., Both, R.A., Arribas, A., Boyce, A.J., Mangas, Martin-Izard, A., 2003. Geology and metallogenic evolution of the polymetallic deposits of the Alcuia Valley mineral field, Eastern Sierra Morena, Spain. *Economic Geology* 98, 577–605.
- Palero-Fernández, F.J., Martín-Izard, A., 2005. Trace element contents in galena and sphalerite from ore deposits of the Alcuia Valley mineral field (Eastern Sierra Morena, Spain). *Journal of Geochemical Exploration* 86, 1–25.
- Penczak, R.S., Mason, R., 1999. Characteristics and origin of Archean premetamorphic hydrothermal alteration at the Campbell Gold Mine, Northwestern Ontario, Canada. *Economic Geology* 94, 507–528.
- Perelló, J.A., 1994. Geology, porphyry Cu-Au, and epithermal Cu-Au-Ag mineralisation of the Tombulilato district, North Sulawesi, Indonesia. *Journal of Geochemical Exploration* 50, 221–256.
- Putz, H., Paar, W.H., Topa, D., Makovicky, E., Roberts, A.C., 2006. Catamarcaite, Cu₆GeWS₈, a new germanium sulfide mineral species from Capillitas, Catamarca, Argentina: description, paragenesis and crystal structure. *Canadian Mineralogist* 44, 1481–1497.
- Putz, H., Paar, W.H., Topa, D., 2009. A contribution to the knowledge of the mineralization at the Mina Capillitas, Catamarca. *Revista de la Asociación de Geológica Argentina* 64, 514–524.
- Richer, M., Tosdal, R.M., Ullrich, T., 2009. Volcanic framework of the Pliocene El Dorado low-sulfidation epithermal gold district, El Salvador. *Economic Geology* 104, 3–18.
- Rieder, M., 1969. Replacement and cockade textures. *Economic Geology* 64, 564–567.
- Sajona, F.G., Izawa, E., Motomura, Y., Imai, A., Sakakibara, H., Watanabe, K., 2002. Victoria carbonate-base metal gold deposit and its significance in the Mankayan mineral district, Luzon, Philippines. *Resource Geology* 52, 315–328.
- Scherbarth, N.L., Spry, P.G., 2006. Mineralogical, petrological, stable isotope, and fluid inclusion characteristics of the Tuvatu gold-silver telluride deposit, Fiji: comparisons with the Emperor Deposit. *Economic Geology* 101, 135–158.
- Schroll, E., Schulz, O., Pak, E., 1983. Sulphur isotope distribution in the Pb-Zn-deposit Bleiberg (Carinthia, Austria). *Mineralium Deposita* 18, 17–25.
- Schütfort, E.G., 2001. The genesis of the San Vicente lead zinc rhythmite deposit, Peru – a petrologic, geochemical, and sulfur isotope study. M.Sc. Thesis, Oregon State University.
- Servida, D., Moroni, M., Ravagnani, D., Rodeghiero, F., Venerandi, I., De Capitani, L., Grieco, G., 2010. Phreatic sulphide bearing quartz breccias between crystalline basement and Collio formation (Southern Alps, Italy). *Italian Journal of Geosciences* 129, 223–236.
- Shelton, K.L., So, C.-S., Haeussler, G.T., Chi, S.-J., Lee, K.-Y., 1990. Geochemical studies of the

- Tongyoung gold-silver deposits, Republic of Korea: evidence of meteoric water dominance in a Te-bearing epithermal system. *Economic Geology* 85, 1114–1132.
- Shikazono, N., 1985. Mineralogical and fluid inclusion features of rock alterations in the Seigoshi gold-silver mining district, western part of the Izu Peninsula, Japan. *Chemical Geology* 49, 213–230.
- Shimizu, T., Matsueda, H., Ishiyama, D., Matsubaya, O., 1998. Genesis of epithermal Au-Ag mineralization of the Koryu Mine, Hokkaido, Japan. *Economic Geology* 93, 303–325.
- Simmons, S.F., Browne, P.R.L., 1990. Mineralogic, alteration and fluid-inclusion studies of epithermal gold-bearing veins at the Mt. Muro Prospect, Central Kalimantan (Borneo), Indonesia. *Journal of Geochemical Exploration* 35, 63–103.
- Simmons, S.F., Gemmell, J.B., Sawkins, F.J., 1988. The Santo Nino silver-lead-zinc vein, Fresnillo District, Zacatecas, Mexico: Part II. Physical and chemical nature of ore-forming solutions. *Economic Geology* 83, 1619–1641.
- Sims, P.K., Hotz, P.E., 1951. Zinc-lead deposit at Shawangunk Mine, Sullivan County, New York. *USGS Bulletin* 978-D.
- Skirrow, R.G., Camacho, A., Lyons, P., Pieters, P.E., Sims, J.P., Stuart-Smith, P.G., Miró, R., 2000. Metallogeny of the southern Sierras Pampeanas, Argentina: geological, ^{40}Ar - ^{39}Ar dating and stable isotope evidence for Devonian Au, Ag-Pb-Zn and W ore formation. *Ore Geology Reviews* 17, 39–81.
- So, C.-S., Park, M.-E., Shelton, K.L., Seidemann, D.E., 1984. Geology and geochemistry of the Sambo Pb-Zn deposit, Republic of Korea. *Economic Geology* 79, 656–670.
- Soechting, W., Rubinstein, N., Godeas, M., 2008. Identification of ammonium-bearing minerals by shortwave infrared reflectance spectroscopy at the Esquel gold deposit, Argentina. *Economic Geology* 103, 865–869.
- Sperling, H., 1973. Die Erzgänge des Erzbergwerks Grund (Silbernaaler Gangzug, Bergwerksglucker Gang und Laubhütter Gang). *Monographien der deutschen Blei-Zink Erzlagerstätten 3 H.2*, Geologisches Jahrbuch D, Schweizerbarth, Stuttgart.
- Spurr, J.E., 1926. Successive banding around rock fragments in veins. *Economic Geology* 21, 519–537.
- Squires, G.C., 2005. Gold and antimony occurrences of the Exploits subzone and Gander zone: a review of recent discoveries and their interpretation. Newfoundland and Labrador Department of Natural Resources Geological Survey Report 05-1, 223–237.
- Stanley, C.J., Halls, C., Camm, G.S., James, J., 1990. Gold-antimony mineralization at Loddiswell, Devon, UK. *Terra Nova* 2, 224–231.
- Subías, I., Moritz, R., Fernández-Nieto, C., 1998. Isotopic composition of strontium in the Valle de Tena (Spanish Central Pyrenees) fluorite deposits: relevance for the source of elements and genetic significance. *Mineralium Deposita* 33, 416–424.
- Tamas, C.G., Milési, J.-P., 2003. Hydrothermal breccia pipe structures – general features and genetic criteria – II. Phreatic breccias. *Studia Universitatis Babeş-Bolyai, Geologia* 48, 55–66.
- Tarnocai, C.A., Hattori, K., Stubens, T.C., 1998. Metamorphosed Archean epithermal Au-As-Sb-Zn-(Hg) vein mineralization at the Campbell Mine, northwestern Ontario – a discussion. *Economic Geology* 93, 683–688.
- Tritlla, J., Cambrubi, A., Morales-Ramírez, J.M., Iriondo, A., Corona-Esquivel, R., González-Partida, E., Levresse, G., Carrillo-Chávez, A., 2004. The Ixtacamaxtitlán kaolinite deposit and sinter (Puebla State, Mexico): a magmatic-hydrothermal system telescoped by a shallow paleoaquifer. *Geofluids* 4, 329–340.
- Tritlla, J., Levresse, G., 2006. Comments on "(U-Th)/He dating of fluorite: application to the La Azul fluorspar deposit in Taxco mining district, Mexico" by Pi et al. (*Mineralium Deposita* 39: 976 – 982). *Mineralium Deposita* 41, 296–299.
- Van Alstine, R.E., 1944. The fluorspar deposits of St. Lawrence, Newfoundland. *Economic Geology* 39, 109–132.

- Volkov, A.V., Prokofev, V.Y., 2011. Formation conditions and composition of ore-forming fluids in the Promezhutochnoe gold and silver deposit (Central Chukchi Peninsula, Russia). *Russian Geology and Geophysics* 52, 1448–1460.
- Voudouris, P., Melfos, V., Spry, P.G., Bonsall, T., Tarkian, M., Economou-Eliopoulos, M., 2008. Mineralogical and fluid inclusion constraints on the evolution of the Plaka intrusion-related ore system, Lavrion, Greece. *Mineralogy and Petrology* 93, 79–110.
- Wake, B.A., Taylor, G.R., 1988. Major's Creek, N.S.W., Australia – A Devonian epithermal gold deposit. *Mineralium Deposita* 23, 239–246.
- Watson, K.D.P., 1943. Colloform sulphide veins of Port au Port peninsula, Newfoundland. *Economic Geology* 38, 621–647.
- Weissenbach, C.G.A., 1836. *Abbildungen merkwürdiger Gangverhältnisse aus dem sächsischen Erzgebirge*. Leopold Voss, Leipzig.
- Wilbur, J.S., Mutschler, F.E., Friedman, J.D., Zartman, R.E., 1990. New chemical, isotopic, and fluid inclusion data from zinc-lead-copper veins, Shawangunk Mountains, New York. *Economic Geology* 85, 182–196.
- Wilkinson, J.J., Lee, M.J., 2003. Cementation, hydrothermal alteration, and Zn-Pb mineralization of carbonate breccias in the Irish Midlands: Textural evidence from the Cooleen Zone, near Silvermines, County Tipperary – a reply. *Economic Geology* 98, 191–193.
- Willan, R.C.R., 1992. Preliminary field observations on peperites and hydrothermal veins and breccias on Livingston Island, South Shetland Islands. *Antarctic Science* 4, 109–110.
- Willan, R.C.R., 1994. Structural setting and timing of hydrothermal veins and breccias on Hurd Peninsula, South Shetland Islands: a possible volcanic-related epithermal system in deformed turbidites. *Geological Magazine* 131, 465–483.
- Willan, R.C.R., Spiro, B., 1996. Sulphur sources for epithermal and mesothermal veins in Cretaceous-Tertiary magmatic-arc rocks, Livingston Island, South Shetland Islands. *Journal of the Geological Society* 153, 51–63.
- Wise, J.M., 2005. Undulatory silver-rich polymetallic veins of the Castrovirreyna District, Central Peru: Fault growth and mineralization in a perturbed local stress field. *Economic Geology* 100, 689–705.
- Wright, V., Woodcock, N.H., Dickson, J.A.D., 2009. Fissure fills along faults: Variscan examples from Gower, South Wales. *Geological Magazine* 146, 890–902.